

SUPPORTING INFORMATION

Red light-triggered photoreduction on a nucleic acid template

Subrata Dutta, Jennifer Rühle, Margot Schikora, Nina Deussner-Helfmann, Mike Heilemann, Timofei Zatsepin, Patrick Duchstein, Dirk Zahn, Günther Knör and Andriy Mokhir

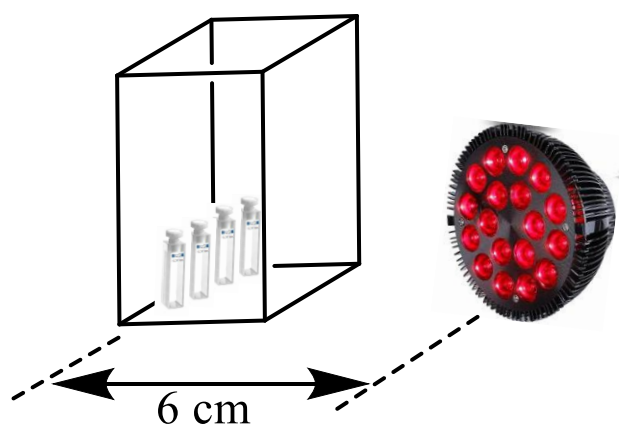
Content

General	p. S1-S2
Synthesis of Sn(IV) complex of pyropheophorbide a	p. S2-S4
Synthesis of S1-S4	p. S5-S12
Additional spectroscopic data (non-templated chemistry)	p. S12-S17
Molecular dynamics simulations	p. S17-S19
Photoreduction of fluorescein and azides	p. S20-S21
Synthesis of DNA and PNA conjugates	p. S21-S26
Additional data (templated chemistry)	p. S26-32
References	p. 33

General

Commercially available chemicals of the best quality from Sigma-Aldrich (Germany) were obtained and used without purification. The reagents for DNA synthesis were obtained either from Sigma-Aldrich (Germany) or Link Technologies (UK). HPLC-purified DNAs were purchased either from IBA GmbH (Germany) or Sigma Aldrich (Germany). MALDI-TOF mass spectra were recorded on either a Bruker BIFLEX III or a Shimadzu Axima Confidence MALDI-TOF mass spectrometers. The matrix mixture was prepared from 2,4,6-trihydroxyacetophenone (THAP, 0.3 M in acetonitrile) and diammonium citrate (0.1 M in water), 2/1, v/v. Samples for mass spectrometry were prepared by a dried droplet method using 1/2 probe/matrix ratio (v/v). Preparative and analytical HPLC was performed at 22 °C on a Shimadzu liquid chromatograph equipped with a UV-detector and a Macherey-Nagel Nucleosil C18 250 x 4.6 mm column, using specified gradients. UV-visible spectra were measured on a JASCO V-550 UV-Vis

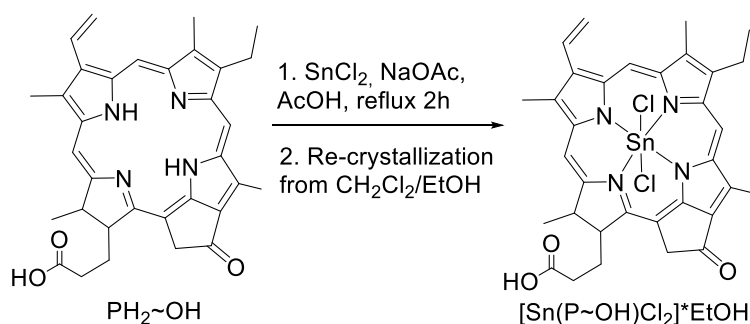
spectrophotometer or a Cary 100 UV-vis from Agilent Technologies or a mobile Lambda Bio+ Photometer. For measurements 1 cm optical path quartz cuvettes (Hellma GmbH, Germany) with a sample volume of 0.1 mL or 0.5 mL, or disposable 70 μ L cuvettes, were used. All photochemical experiments were conducted in the set up outlined in Scheme S1. We used a box opened to light from one side and closed from other sides. The interior of the box was covered with aluminium. Cuvettes were placed inside the box. The distance between the light source and the cuvettes was set to 6 cm. The cuvettes were irradiated with red LED lamp compiled of eighteen 2-watt super bright red LEDs ($\lambda = 660$ nm, Flux = 1086 lm, efficacy: 56.6 lm/w; half width at half maximum = 26.4 nm). Both the box and the light source were fully covered with aluminium foil during illumination.



Scheme S1. A set-up used for the photochemical reactions.

Synthesis

Tin(IV)(pyropheophorbide a)Cl₂ ([Sn(P~OH)Cl₂]. Pyropheophorbide a (PH₂~OH, 175 mg, 0.327 mmol) and sodium acetate (133.32 mg, 1.6 mmol) were dissolved in glacial acetic acid (10 mL). Separately, anhydrous SnCl₂ (411 mg, 2.17 mmol) was dissolved in dimethylformamide (DMF, 0.5 mL) and slowly added to the PH₂~OH solution. The reaction mixture was stirred at 110 °C for 90 min. During the reaction time a constant air flow through the reaction mixture was provided. The reaction was cooled to 22 °C and acetic acid was removed under reduced pressure. The obtained residue was dissolved in CH₂Cl₂ (10 mL) and washed with 1M aqueous hydrochloric acid (4 x 15 mL). The organic layer was collected and dried over anhydrous sodium sulfate and the solvent



Scheme S2. Synthesis of [Sn(P~OH)Cl₂].

was removed under reduced pressure (0.01 bar). The crude product was purified by recrystallization from CH₂Cl₂ (DCM) and ethanol. For this purpose the product was dissolved in DCM (~ 2 mL) and layered with the same amount

of ethanol. After 15 min of standing at 22 °C, the two layers were mixed with one swirl and the mixture was put in the freezer for precipitation overnight. The filtered sample was dried in vacuum (0.1 mbar) until the constant weight was achieved. The procedure yielded [Sn(P~OH)Cl₂]*EtOH as a dark green solid (204 mg, 0.28 mmol, 86%). ¹H-NMR (500 MHz, CDCl₃): δ = 9.94 (s, 1H), 9.76 (s, 1H), 8.79 (s, 1H), 7.95 (dd, 1H, J =17.94, 11.62 Hz), 6.34 (d, 1H, J=16.93 Hz), 6.24 (d, 1H, J=11.62 Hz), 5.36 – 5.19 (m, 2H), 4.8 – 4.72 (m, 1H), 4.6 – 4.55 (m, 1H), 3.87 (q, 2H, J= 7.49 Hz), 3.73 (s, 3H,), 3.41 (s, 6H,), 2.82 – 2.72 (m, 1H), 2.67 – 2.57 (m, 1H), 2.54 – 2.45 (m, 1H), 2.38 – 2.29 (m, 1H), 1.95 (d, 3H, J=7.33 Hz), 1.81 (t, 3H, J=7.71 Hz). ¹³C-NMR (125 MHz, CDCl₃): δ (ppm) = 194.33, 177.12, 165.25, 157.109, 154.07, 150.30, 146.61, 145.56, 145.37, 143.36, 142.63, 141.09, 140.08, 137.92, 135.55, 135.42, 133.03, 128.45, 124.08, 106.93, 104.72, 100.05, 92.28, 50.24, 48.56, 48.23, 29.23, 23.30, 19.70, 17.13, 12.90, 12.17, 11.15. HR-MS (APPI+), m/z: calculated for C₃₃H₃₂ClN₄O₃Sn [M-Cl]⁺ 687.1179, found 687.1180. C, H, N analysis: calculated for C₃₃H₃₂Cl₂N₄O₃Sn*EtOH (%) – C 54.71, H 4.99, N 7.29. found – C 54.31, H 4.87, N 7.20.

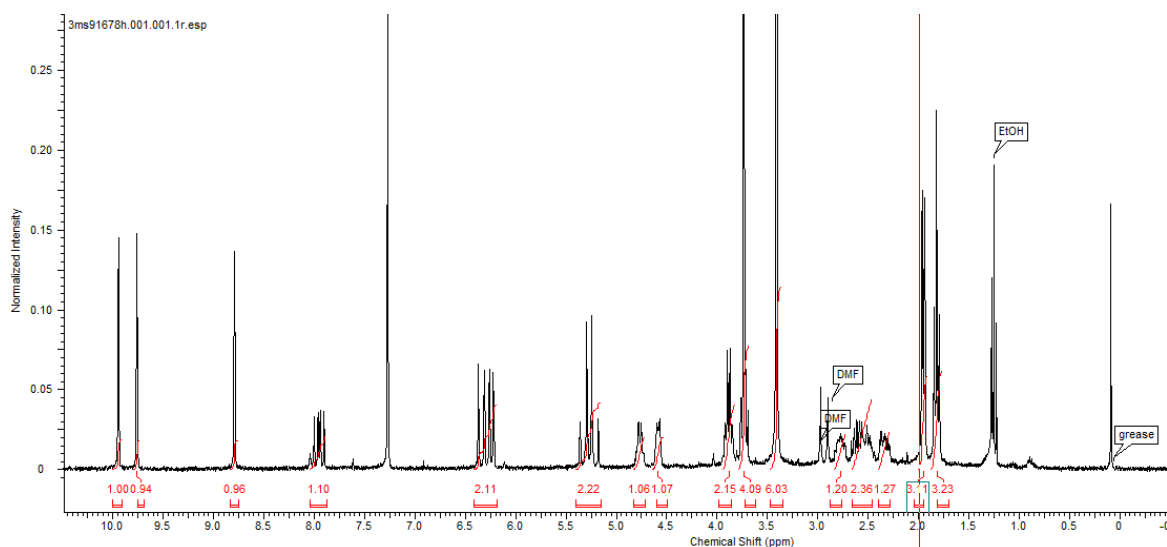


Figure S1. ¹H NMR spectrum of [Sn(P~OH)Cl₂]*EtOH.

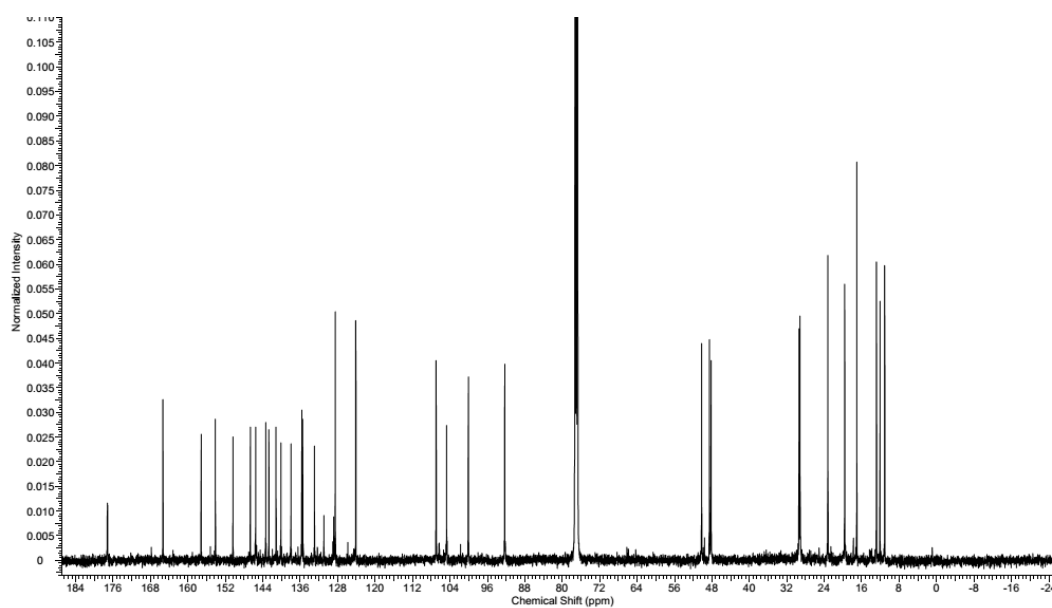


Figure S2. ^{13}C NMR spectrum of $[\text{Sn}(\text{P}\sim\text{OH})\text{Cl}_2]\cdot\text{EtOH}$.

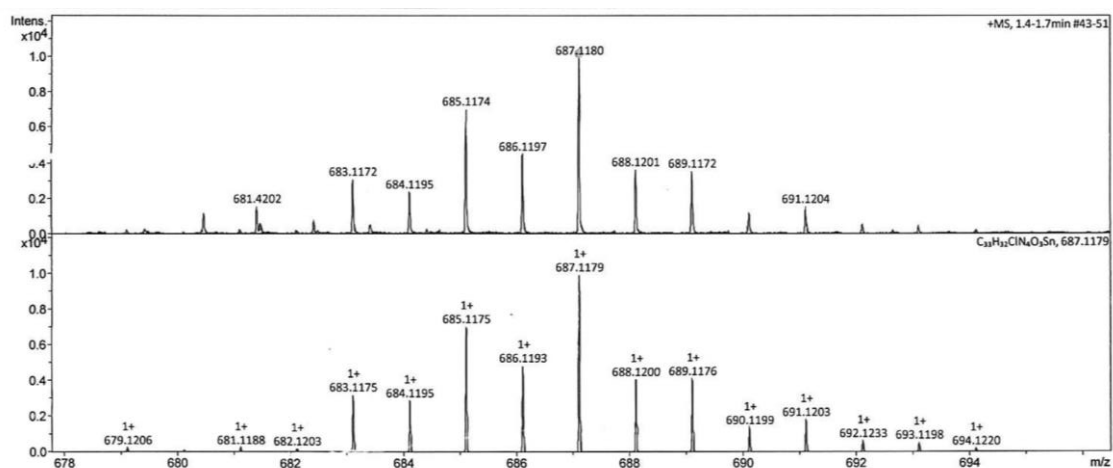
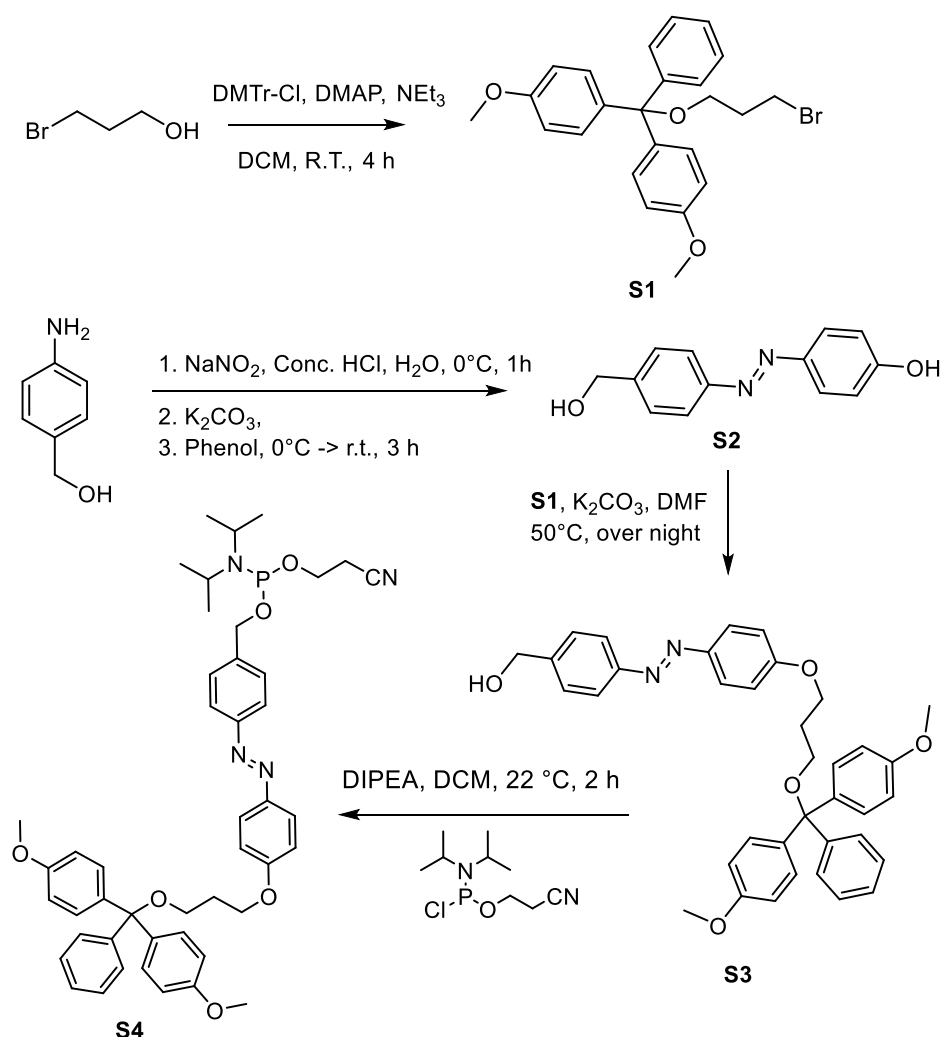


Figure S3: High resolution mass spectrum of $[\text{Sn}(\text{P}\sim\text{OH})\text{Cl}_2]\cdot\text{EtOH}$.

Intermediate S1 (Scheme S3)



Scheme S3. Outline of synthesis of phosphoramidite **S4**.

In a dry Schlenk flask dimethoxytriphenylmethylchloride (DMTr-Cl) (787 mg, 2.32 mmol) and 4-dimethylaminopyridine (DMAP, 27 mg, 0.220 mmol) were dissolved in 10 mL anhydrous dichloromethane (DCM) under a nitrogen atmosphere. Then first, 3-bromopropan-1-ole (200 μ L, 2.21 mmol) was added and finally triethylamine (310 μ L, 2.22 mmol) was added slowly whereas the colour changed from red to colourless. After stirring for 6 h at 22 °C, the reaction solution was poured onto water (20 mL). The aqueous phase was extracted three times with DCM (20 mL), the combined organic phases were dried over anhydrous MgSO₄ and filtered. The solvent was evaporated, and the crude product was purified by column chromatography with a 10:1 mixture of cyclohexane/ethylacetate (v/v) to give **S1** as colourless crystals (878 mg, 1.99 mmol, 90% yield). ¹H-NMR (300 MHz, CDCl₃) δ (ppm) = 7.46 – 7.40 (m, 2H), 7.35 – 7.30 (m, 4H), 7.30 – 7.26 (m, 2H), 7.25 – 7.18 (m, 1H), 6.87 – 6.79 (m, 4H), 3.80 (s, 6H), 3.57 (t,

J = 6.8 Hz, 2H), 3.21 (t, J = 5.9 Hz, 2H), 2.18 – 2.04 (m, 2H), 1.43 (s, 6H). ¹³C-NMR (101 MHz, CDCl₃) δ (ppm) = 158.56, 145.19, 136.42, 130.15, 128.27, 127.90, 126.85, 113.20, 86.05, 61.17, 55.35, 33.67, 31.02. HR-MS (APPI+), m/z: calculated for C₂₄H₂₅BrO₃ [M+H]⁺ 440.0982, found 440.0979.

Intermediate S2

In a round bottom flask 4-aminobenzylalcohol (1.50 g, 12.18 mmol) was dissolved in water (22 mL) while stirring and was then cooled to 0°C with an ice bath. After addition of conc. HCl-solution (2.6 mL) a cooled solution of NaNO₂ (0.88 g, 12.78 mmol) in water (6 mL) was added dropwise. The reaction solution was stirred further at 0°C for 1 h. Then, a solution of phenol (1.20 g, 12.79 mmol) and K₂CO₃ (0.88 g, 12.78 mmol) in water (20 mL) was added dropwise. When the reaction solution couldn't be stirred anymore due to precipitation of product more water (10 mL) was added directly to the reaction solution. After stirring for 2 h at 0°C the ice bath was removed and diluted acetic acid (2:1 H₂O/99% glacial acetic acid, v/v) was added until a pH of ~5 was reached (around 24 mL were needed). The precipitated product was then vacuum filtered, washed with water and small amounts of MeOH. Drying in high vacuum gave **S2** as orange crystals (2.72 g, 11.92 mmol, 98% yield). ¹H-NMR (400 MHz, DMSO-d₆) δ (ppm) = 10.26 (s, 1H), 7.79 (dd, J = 8.6, 1.7 Hz, 4H), 7.49 (d, J = 8.4 Hz, 2H), 6.94 (d, J = 8.8 Hz, 2H), 5.33 (s, 1H), 4.58 (s, 2H). ¹³C-NMR (101 MHz, DMSO-d₆) δ (ppm) = 160.96, 151.19, 145.44, 127.27, 124.89, 122.14, 116.10, 62.69. HR-MS (ESI+), m/z: calculated for C₁₃H₁₂N₂O₂ [M+H]⁺ = 229.0972, found 229.0978.

Intermediate S3

A Schlenk flask filled with K₂CO₃ (133 mg, 0.962 mmol) and a condenser were heated by using hot air heat gun under vacuum. After the apparatus was cooled down to 22 °C it was charged with N₂. Then, compound **S2** (184 mg, 0.806 mmol) and **S1** (415.8 mg, 0.942 mmol) were added and the resulting mixture was dissolved in anhydrous DMF (1 mL). While stirring, the reaction solution was heated over night at 50°C. Afterwards the reaction solution was poured onto water (10 mL). The aqueous phase was extracted with several portions of DCM (10 mL) until the extract turned colourless. The organic phases were combined, dried over anhydrous Na₂SO₄ and filtered. After removal of the solvent the crude product was purified by column chromatography with a 2:1 mixture of cyclohexane/DCM (v/v) as eluent on Allox (with activity 3) to give **S3** as an orange solid

with 90% yield (425 mg, 0.722 mmol). $^1\text{H-NMR}$ (400 MHz, DMSO- d_6) δ (ppm) = 7.88 (d, J = 9.0 Hz, 2H), 7.82 (d, J = 8.4 Hz, 2H), 7.51 (d, J = 8.5 Hz, 2H), 7.37 (d, J = 7.2 Hz, 2H), 7.28 (t, J = 7.5 Hz, 2H), 7.23 (t, J = 8.8 Hz, 5H), 7.09 (d, J = 9.0 Hz, 2H), 6.85 (d, J = 8.9 Hz, 4H), 5.34 (s, 1H), 4.63 – 4.54 (m, 2H), 4.21 (t, J = 6.0 Hz, 2H), 3.72 (s, 6H), 3.17 (t, J = 6.0 Hz, 2H), 2.01 (p, J = 5.3, 4.7 Hz, 2H). $^{13}\text{C-NMR}$ (101 MHz, DMSO- d_6) δ (ppm) = 161.65, 158.46, 151.40, 146.60, 146.10, 145.56, 136.33, 130.08, 128.25, 127.56, 127.06, 124.92, 122.57, 115.50, 113.59, 85.83, 62.96, 59.78, 29.72. HR-MS (APPI+), m/z : calculated for $\text{C}_{37}\text{H}_{36}\text{N}_2\text{O}_5$ $[\text{M}+\text{H}]^+$ = 589.2697, found 589.2705.

Phosphoramidite S4

In a vacuum dried and with N_2 charged Schlenk flask **S3** (268 mg, 0.455 mmol) and N,N -diisopropylethylamine (DIPEA, 0.36 mL, 2.017 mmol) were dissolved in anhydrous DCM (5 mL). Then, 2-cyanoethyl- N,N -diisopropylchlorophosphoramidite (0.14 mL, 0.627 mmol) was added dropwise and the resulting reaction solution was stirred at 22 °C for 2 h. Subsequently, the reaction solution was poured onto of sat. NaHCO_3 solution (10 mL). The aqueous phase was extracted 3 times with DCM (10 mL), the combined organic phases were dried over anhydrous Na_2SO_4 , filtered and the solvent was removed in vacuo. The crude product was purified under N_2 atmosphere by column chromatography on Allox (activity 3) with a mixture of cyclohexane/DCM 2:1 (v/v) as eluent to give **S4** as orange gel with a yield of 70% (250 mg, 0.317 mmol). $^1\text{H-NMR}$ (300 MHz, Acetone- d_6) δ (ppm) = 7.93 (d, J = 9.0 Hz, 2H), 7.88 (d, J = 8.5 Hz, 2H), 7.59 (d, J = 8.6 Hz, 2H), 7.47 (d, J = 8.2 Hz, 2H), 7.37 – 7.30 (m, 4H), 7.30 – 7.18 (m, 3H), 7.14 – 7.06 (m, 2H), 6.88 – 6.82 (m, 4H), 4.94 – 4.77 (m, 2H), 4.31 (t, J = 6.2 Hz, 2H), 3.99 – 3.85 (m, 2H), 3.77 (s, 6H), 3.75 – 3.63 (m, 2H), 3.31 (t, J = 6.0 Hz, 2H), 2.82 (s, 3H), 2.79 – 2.77 (m, 2H), 2.18 – 2.07 (m, 2H), 1.23 (dd, J = 6.8, 2.6 Hz, 13H). $^{31}\text{P-NMR}$ (122 MHz, Acetone- d_6) δ (ppm) = 148.39, $^{13}\text{C-NMR}$ (76 MHz, Acetone- d_6) δ (ppm) = 162.97, 159.78, 147.92, 146.72, 143.51, 137.47, 131.13, 129.20, 128.76, 127.69, 125.74, 123.50, 116.06, 114.07, 86.99, 66.39, 66.02, 65.78, 60.61, 60.05, 59.80, 55.72, 44.26, 44.09, 25.23, 21.00. MS (MALDI+), m/z : calculated for $\text{C}_{46}\text{H}_{54}\text{N}_4\text{O}_6\text{P}$ $[\text{M}+\text{H}]^+$ = 789.37, found 789.22.

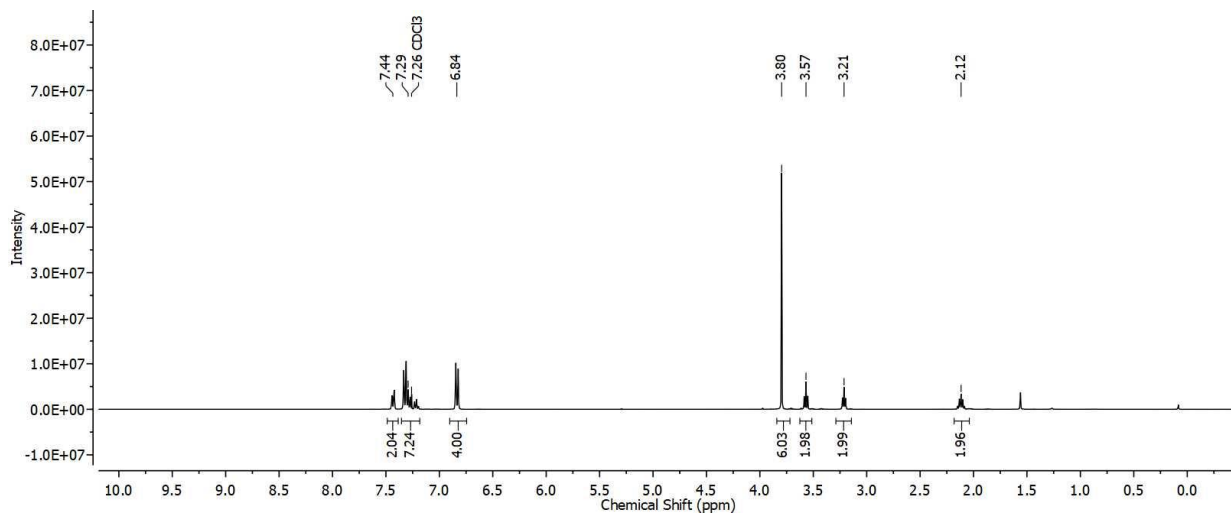


Figure S4. ^1H NMR spectrum of compound S1.

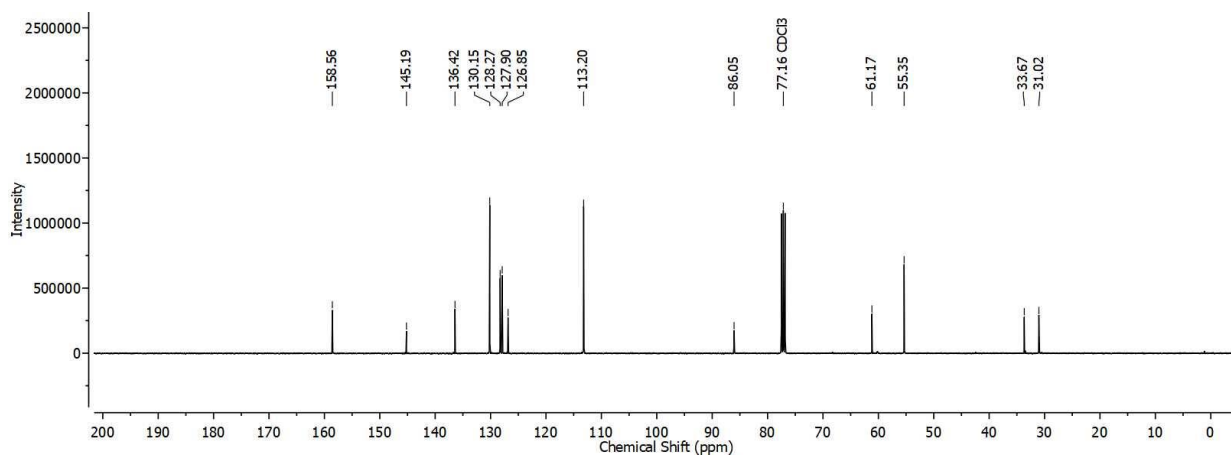


Figure S5. ^{13}C NMR spectrum of compound S1.

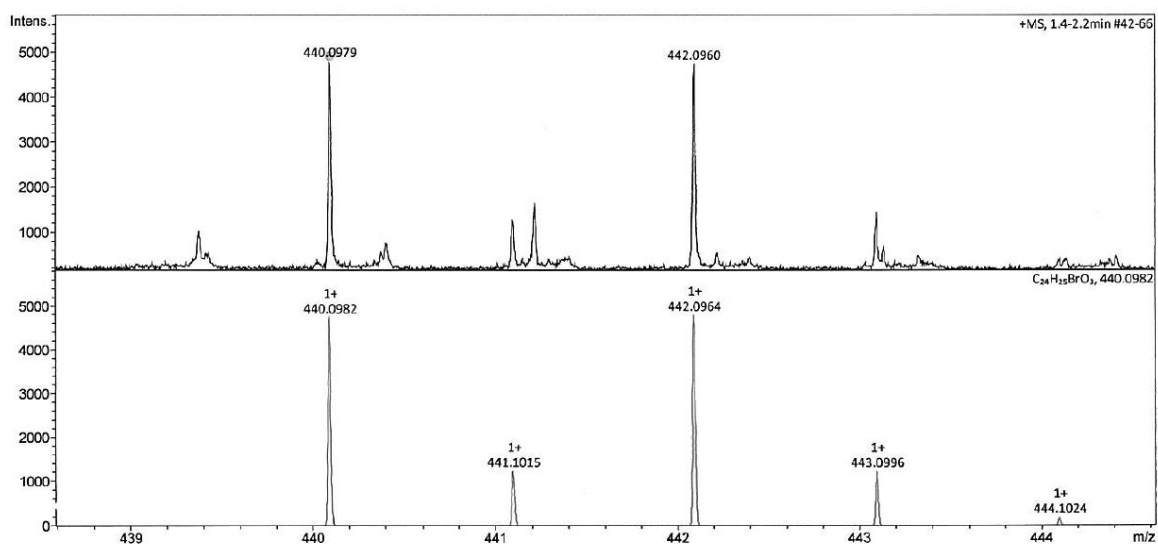


Figure S6: Mass spectrum of compound S1.

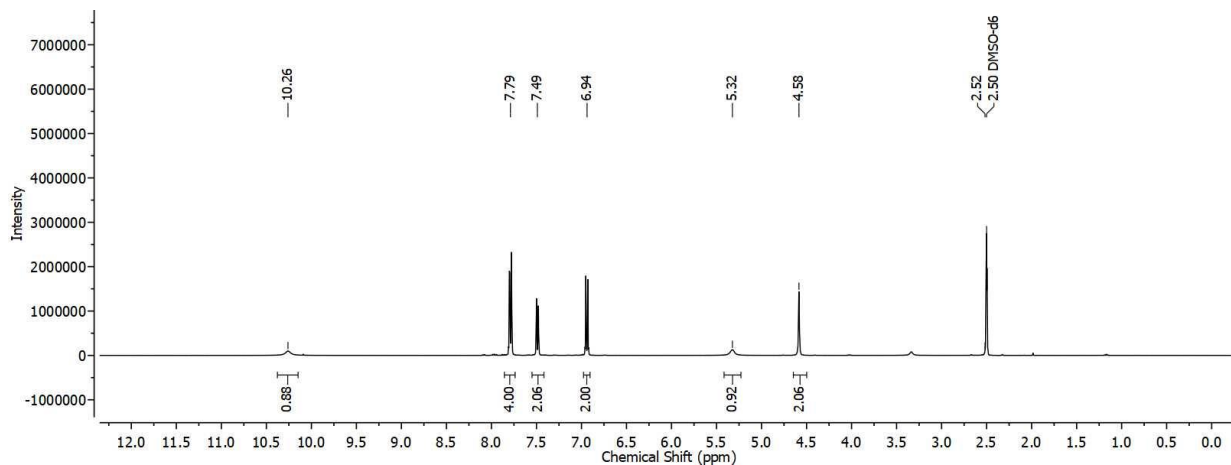


Figure S7. ^1H NMR spectrum of compound S2.

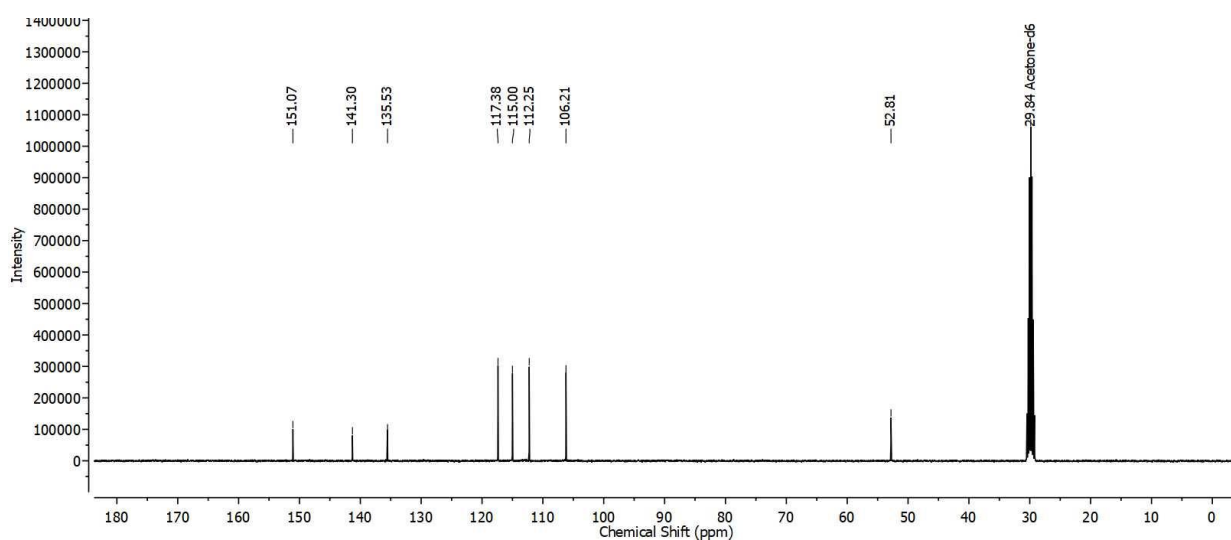


Figure S8. ^{13}C NMR spectrum of compound S2.

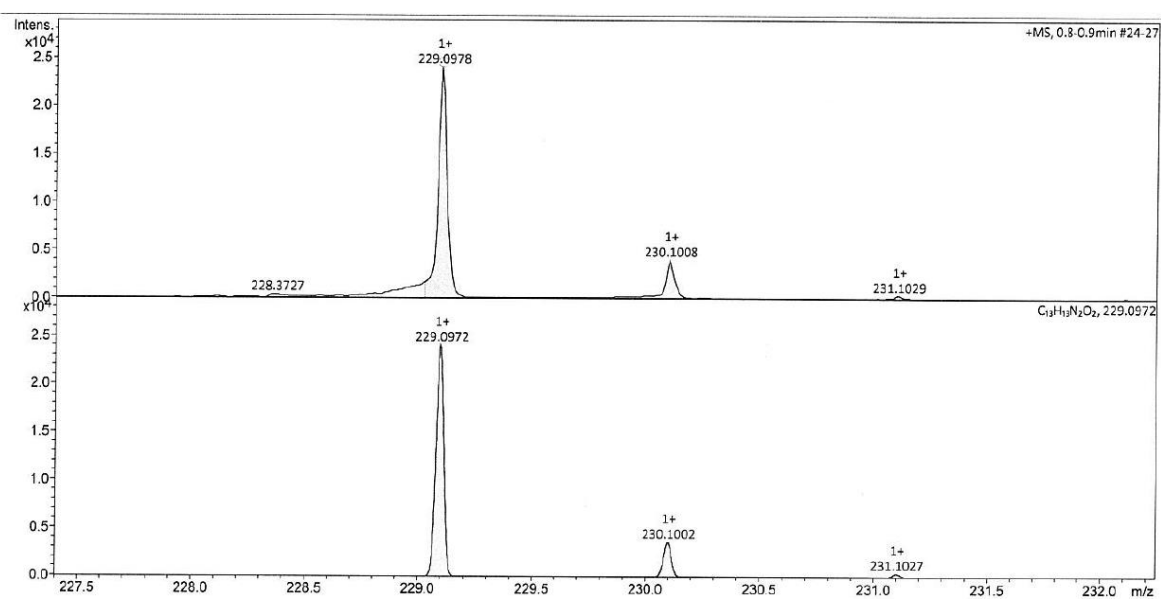


Figure S9: Mass spectrum of compound S2.

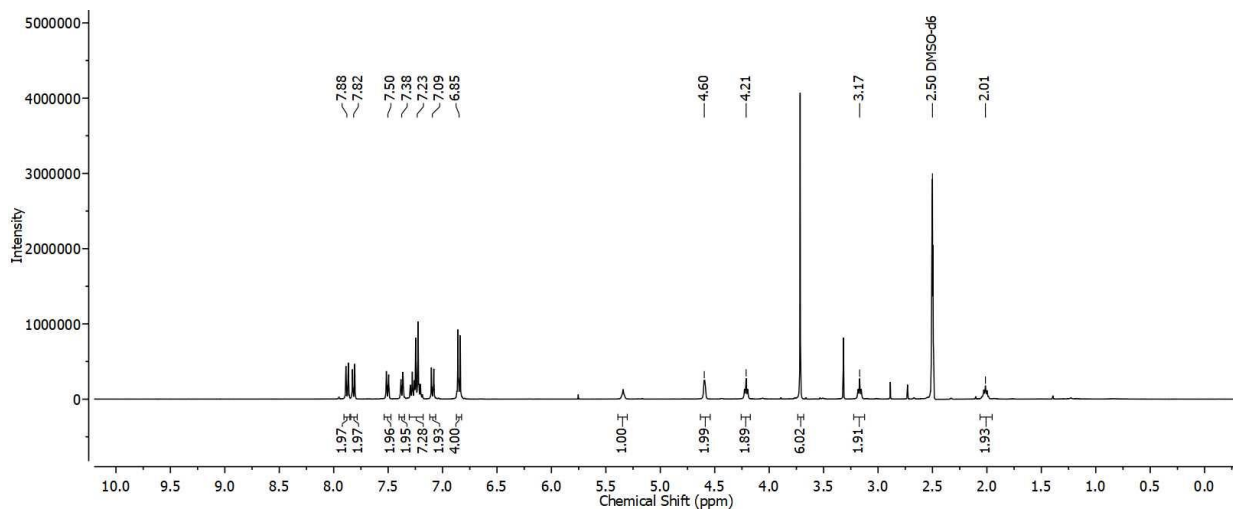


Figure S10. ^1H NMR spectrum of compound **S3**.

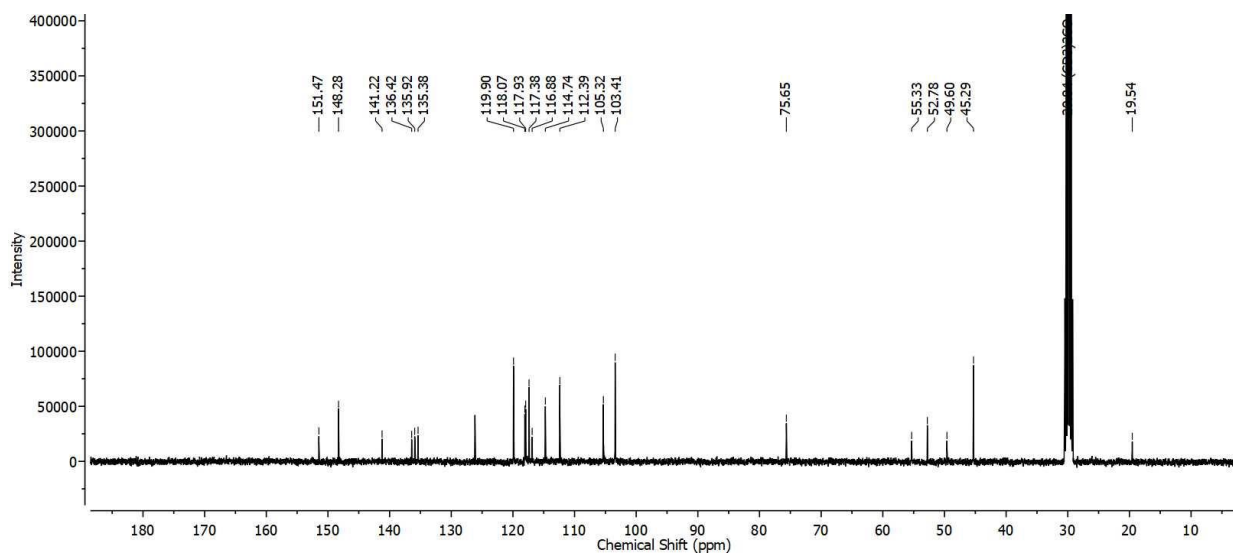


Figure S11. ^{13}C NMR spectrum of compound **S3**.

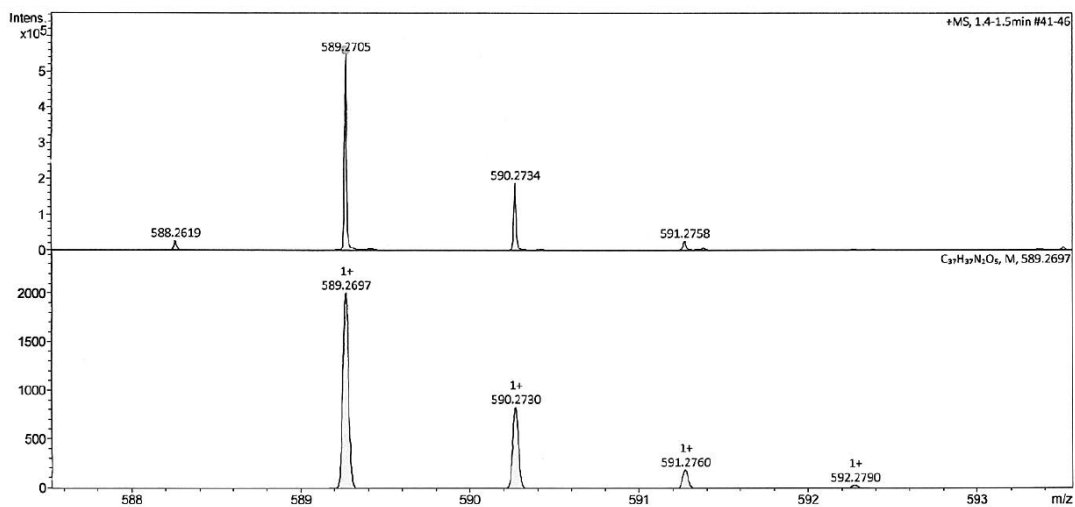


Figure S12: Mass spectrum of compound **S3**.

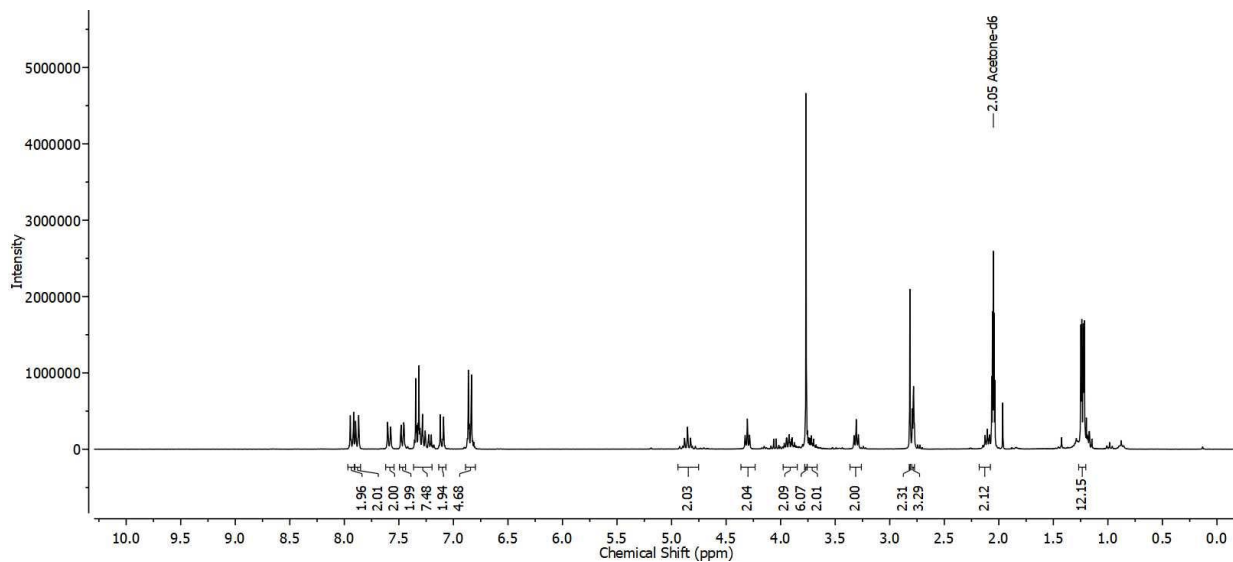


Figure S13. ¹H NMR spectrum of compound S4.

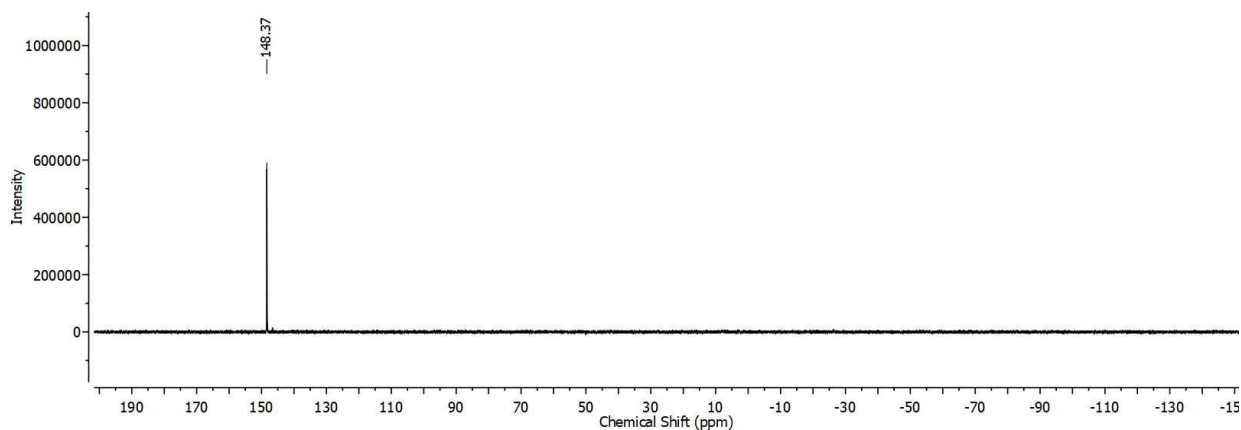


Figure S14. ³¹P NMR spectrum of compound S4.

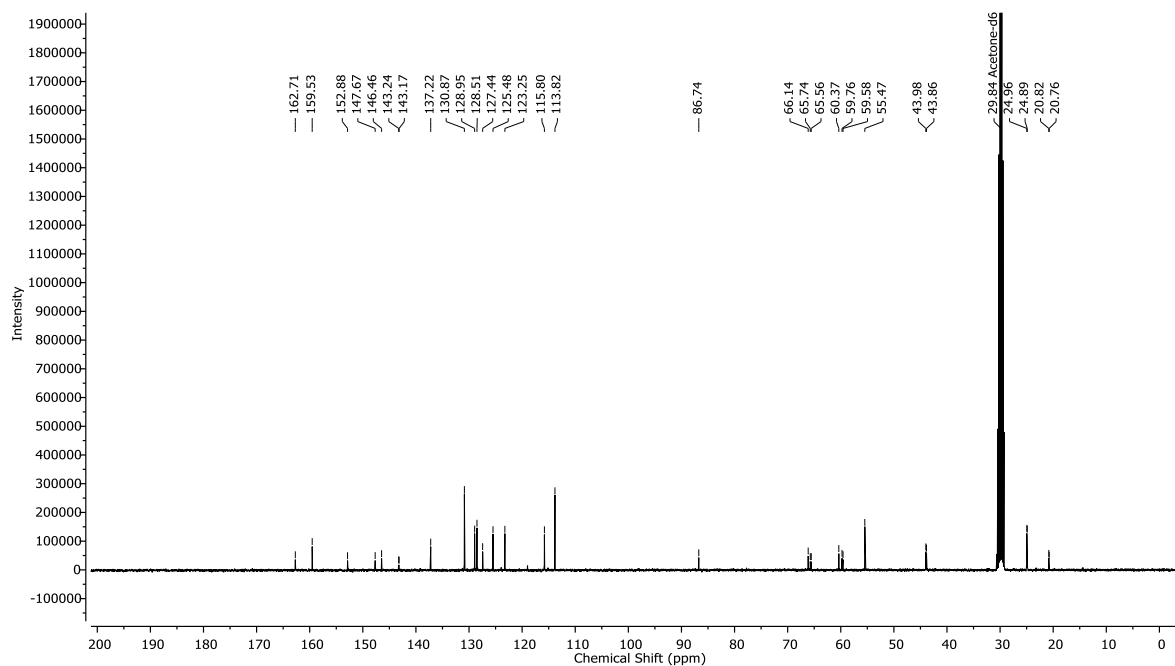


Figure S15. ¹³C NMR spectrum of compound S4.

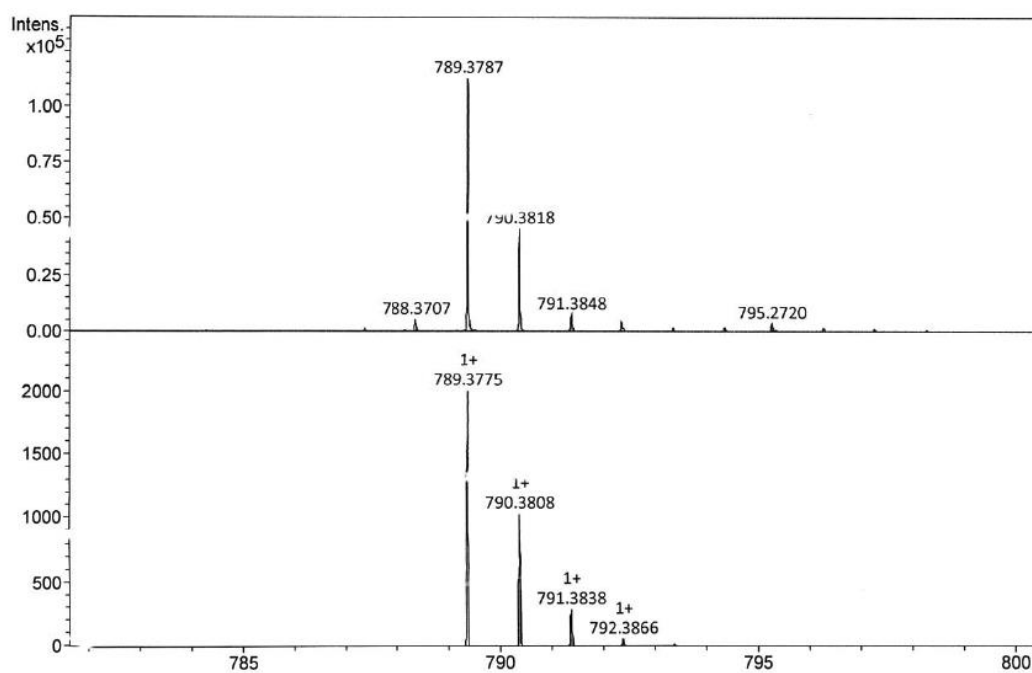


Figure S16: Mass spectrum of compound **S4**.

Additional spectroscopic data (non-templated chemistry)

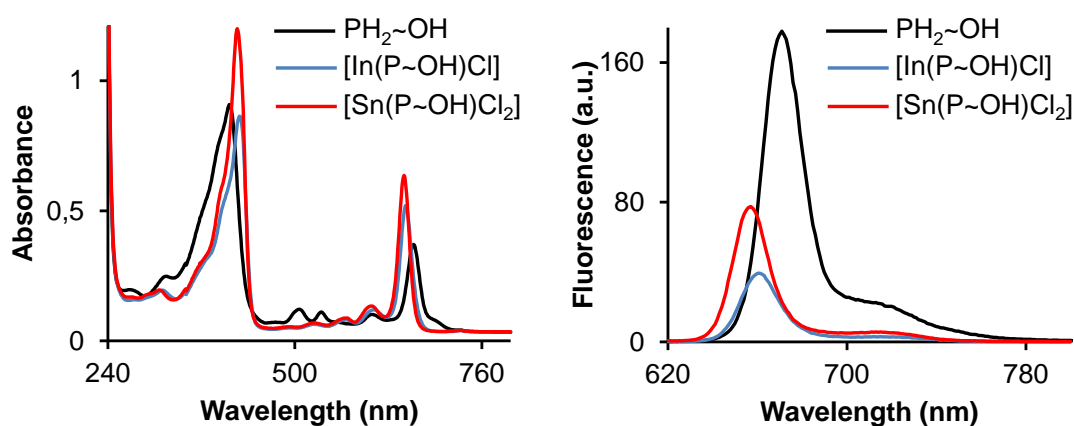


Figure S17. Left plot: UV-visible spectra of pyropheophorbide a ($\text{PH}_2\sim\text{OH}$) and its In(III) ($[\text{In}(\text{P}\sim\text{OH})\text{Cl}]$) and Sn(IV) ($[\text{Sn}(\text{P}\sim\text{OH})\text{Cl}_2]$) complexes; concentration of each compound is $10\ \mu\text{M}$ in CH_3CN . Right plot: Fluorescence spectra of the same compounds ($1\ \mu\text{M}$ in CH_3CN): $\lambda_{\text{ex}}(\text{PH}_2\sim\text{OH})= 410\ \text{nm}$; $\lambda_{\text{ex}}([\text{In}(\text{P}\sim\text{OH})\text{Cl}])= 424\ \text{nm}$; $\lambda_{\text{ex}}([\text{Sn}(\text{P}\sim\text{OH})\text{Cl}_2])= 420\ \text{nm}$. Emission maxima: $\lambda_{\text{em}}(\text{PH}_2\sim\text{OH})= 670\ \text{nm}$; $\lambda_{\text{em}}([\text{In}(\text{P}\sim\text{OH})\text{Cl}])= 660\ \text{nm}$; $\lambda_{\text{em}}([\text{Sn}(\text{P}\sim\text{OH})\text{Cl}_2])= 657\ \text{nm}$

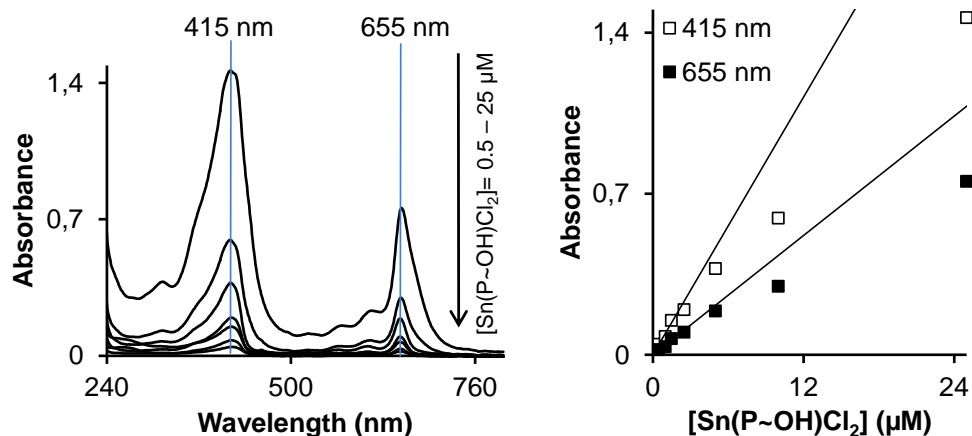


Figure S18. Left plot: UV-visible spectra of [Sn(P~OH)Cl₂] (0.5 – 25 μM, dissolved in aqueous phosphate buffer, 10 mM, pH 7 containing NaCl, 150 mM and 1 % DMSO, v/v). Right plot: Dependence of absorbance A(415 nm) and A(655 nm) from the complex concentration. The initial parts of these dependences are linear as indicated by black solid lines. This is a representative data set. For complex [In(P~OH)Cl] similar effects were observed.

Assaying production of singlet oxygen (¹O₂) in the result of irradiation of catalysts [In(P~OH)Cl] and [Sn(P~OH)Cl₂] with red light both in presence and absence of sodium ascorbate

We used water soluble 1,3-di-(4-carboxyphenyl)isobenzofuran (IBF) for detection of ¹O₂. IBF is a fluorescent compound (λ_{ex}= 430 nm), which reacts with ¹O₂ and forms a colorless product. In particular, IBF (25 μM) and photocatalyst (2 μM) were mixed in phosphate buffer (10 mM, pH 7) containing NaCl (150 mM) and sodium ascorbate (10 mM). A control sample was also prepared lacking ascorbate. These mixtures were irradiated with red light and the bleaching of IBF was observed by fluorescence spectroscopy.

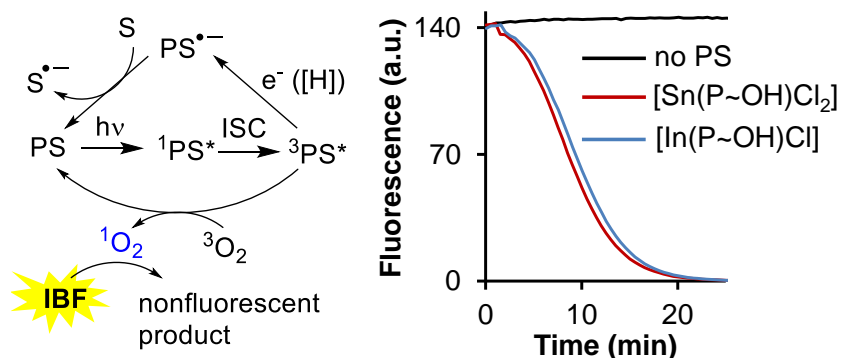


Figure S19. Left plot: A diagram illustrating generation of a triplet state ($^3\text{PS}^*$) upon irradiation of a photosensitizer PS (e.g. $[\text{Sn}(\text{P}\sim\text{OH})\text{Cl}_2]$) with red light and transformation of this state back to the ground state via two possible pathways: (a) the energy transfer to $^3\text{O}_2$ with formation of $^1\text{O}_2$ and (b) the reduction of $^3\text{PS}^*$ in the presence of bulk reductant (e.g. ascorbate) with formation of $\text{PS}^{\bullet-}$ and the further transfer of an electron to the substrate (e.g. BHQ2-R). Right plot: Monitoring generation of $^1\text{O}_2$ (based on the bleaching of isobenzofurane (IBF, $25\ \mu\text{M}$, $\lambda_{\text{ex}} = 430\ \text{nm}$, $\lambda_{\text{em}} = 470\ \text{nm}$) in the presence of $^1\text{O}_2$) upon irradiation of the following solutions with red light: no PS (black curve); with $[\text{Sn}(\text{P}\sim\text{OH})\text{Cl}_2]$ ($2\ \mu\text{M}$, red curve); with $[\text{In}(\text{P}\sim\text{OH})\text{Cl}]$ ($2\ \mu\text{M}$, blue curve); buffer: aqueous phosphate, $10\ \text{mM}$, pH 7 containing NaCl, $150\ \text{mM}$ and $1\ \%$ DMSO, v/v; a.u.= arbitrary units.

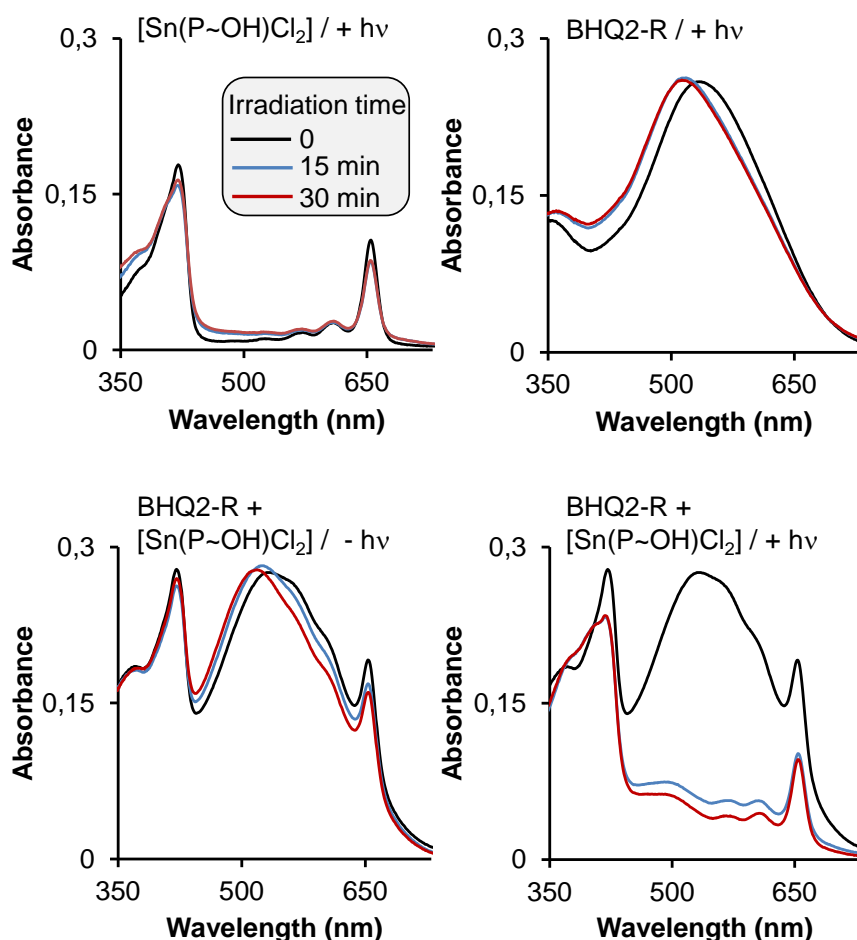


Figure S20. UV-visible spectra of solutions (phosphate buffer, 10 mM, pH 7 containing NaCl, 150 mM, 2 % DMSO (v/v) and sodium ascorbate, 10 mM) of (a) $[\text{Sn}(\text{P}\sim\text{OH})\text{Cl}_2]$ ($2\ \mu\text{M}$), (b) BHQ2-R ($10\ \mu\text{M}$) and (c) a mixture of $[\text{Sn}(\text{P}\sim\text{OH})\text{Cl}_2]$ ($2\ \mu\text{M}$) and BHQ2-R ($10\ \mu\text{M}$) as indicated on the plot. Solutions (a), (b) and (c) were irradiated with red light for 0 (black curves), 15 (blue curves) and 30 min (red curves). These data are labeled “+ $h\nu$ ”. As a control, the solution (c) was also kept in the dark for 30 min: the spectra are labeled “- $h\nu$ ”. Structures of $[\text{Sn}(\text{P}\sim\text{OH})\text{Cl}_2]$ and BHQ2-R are shown in Scheme 1. These are representative data. When $[\text{Sn}(\text{P}\sim\text{OH})\text{Cl}_2]$ was replaced with $[\text{In}(\text{P}\sim\text{OH})\text{Cl}]$ no cleavage of the substrate was obtained. The slight shift of the absorbance maximum of BHQ2-R solution from 535 nm to 520 nm occurs also in the dark. According to electrospray ionization (ESI) mass spectrometry (MS) data, the latter change corresponds to light independent hydrolysis and partial oxidation of the phosphoramidite group, which, however, does not affect the azo dye chromophore of BHQ2-R.

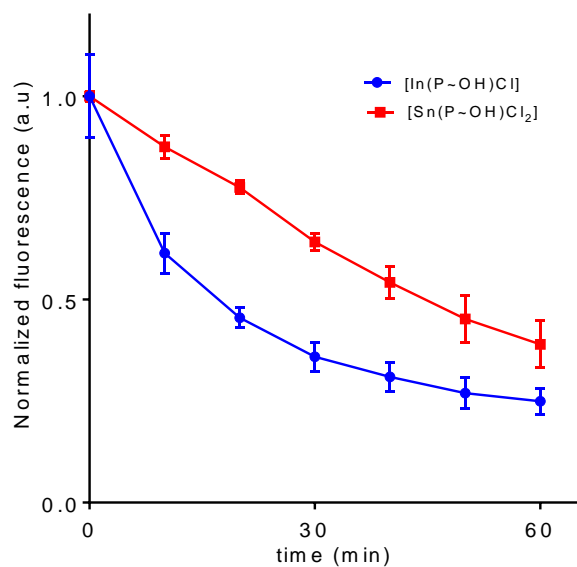


Figure S21: Photostability of [In(P~OH)Cl] and [Sn(P~OH)Cl₂]. Both the sample (1 μ M) were exposed to the red light and fluorescence intensity ($\lambda_{\text{ex}}= 430$ nm, $\lambda_{\text{em}}= 660$ nm) was measured over a period of 60 min. Buffer used: phosphate, 10 mM, pH 7.0, NaCl, 150 mM, sodium ascorbate, 10 mM, 1% DMSO (v/v).

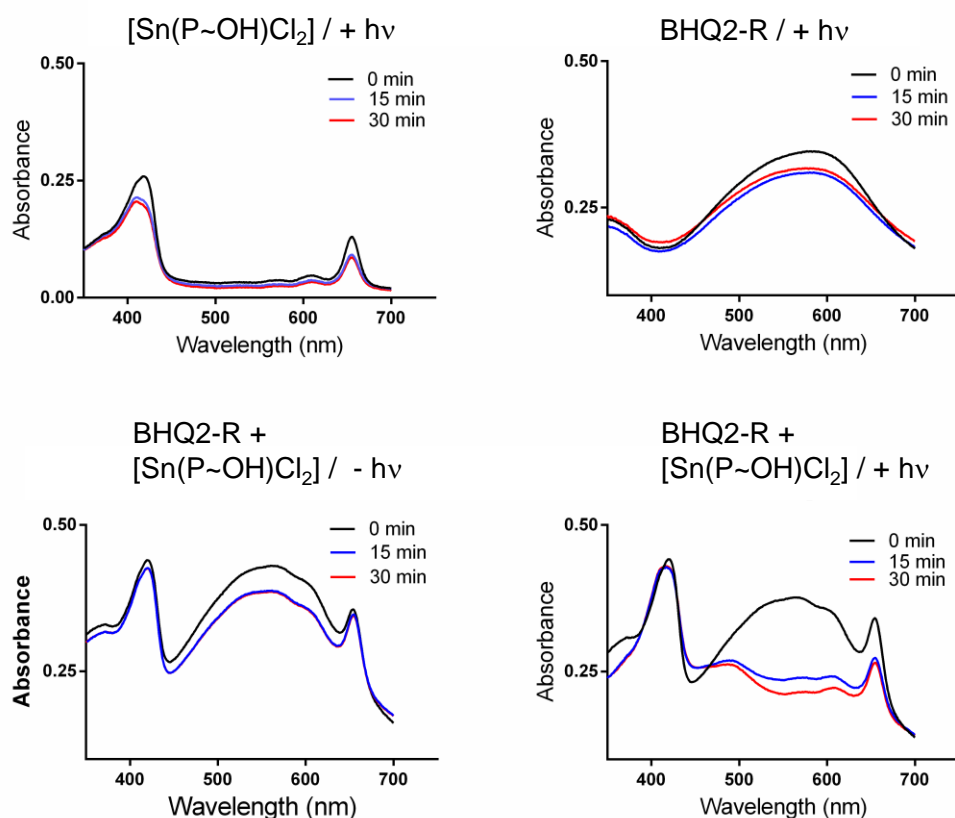


Figure S22. The same as Figure S21, but with BHQ2-R was replaced with BHQ1-R.

Molecular Dynamics Simulations

We set up a cubic simulation box containing the BHQ, PS, 2094 water molecules, and Cl^- ions for charge neutralization as needed. Periodic boundary conditions were enabled, and the box exhibited a length of 3,99 nm in each direction. The underlying force-fields were GAFF2 for P~OH and BHQ with RESP charges, Li/Merz ion parameters for In(III) and Sn(IV) with formal charges, and SPC/Fw water.^{S1-S5} For electrostatic interactions, we employed a damped shifted force coulomb type of potential with a cutoff of 12 Å. The system was first equilibrated for 100 ps and then propagated for 50 ns. Throughout our molecular dynamics runs, ambient conditions were applied and a timestep of 1 fs was used.

The association of BHQ and PS was investigated from direct molecular dynamics simulations starting from separate solutes in solution. After 10-20 ns simulation time, PS and BHQ molecules were directly associated with each other. For both, the In- and the Sn-based PS, we observed BHQ-PS association driven by hydrophobic segregation and π -stacking of the aromatic groups (Figure S23). However, the In-based PS is associated

somewhat laterally to BHQ such that the metallic center is separated from the azo group. On the other hand, the Sn-based PS exhibits a staggered arrangement upon association to the BHQ. This leads to a closer contact of the catalytic site and the azo group. Indeed, the shortest pyridine-azo N-N distances were found as 3.0 and 3.3 Å for the Sn-PS and the In-PS, respectively.

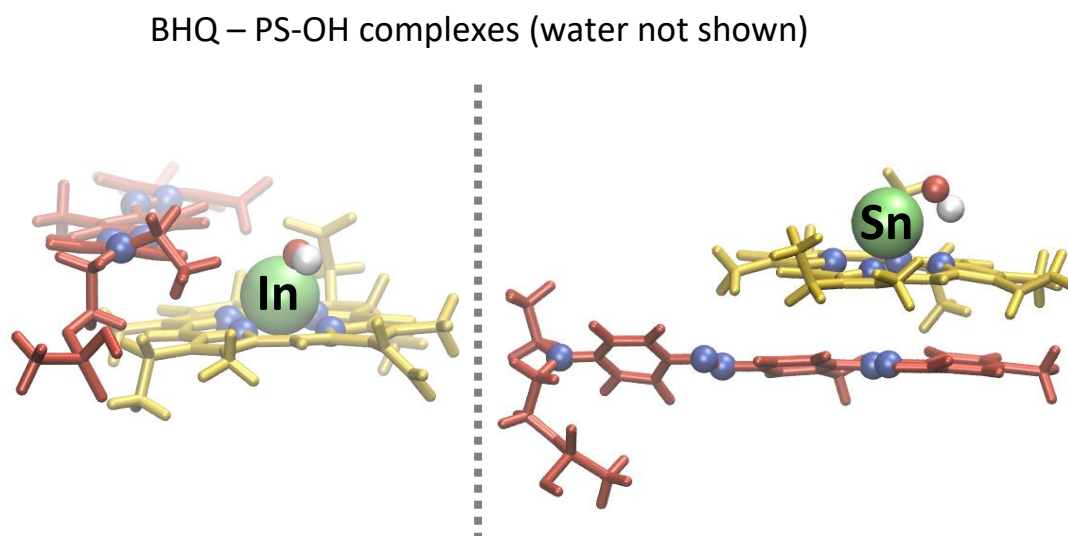


Figure S23. Illustration of the BHQ(red)-PS(yellow) complexes in solution after 50 ns of relaxation. The In(III) (left) and Sn(IV) (right) ions are colored in green and the nitrogen atoms of the azo- and pyridine groups are highlighted in blue. The solvent, including coordinating water is omitted, whilst the OH⁻ ion is shown in red/white. The shortest Sn-N(azo) distance was found as 4.6 Å, whereas the shortest In-N(azo) distance was found as 4.0 Å, respectively. However, considering the atoms involved in possible electron transfer, we must focus on the shortest N(pyridine)-N(azo) distances which were found as 3.0 and 3.3 Å for the Sn-PS and the In-PS, respectively.

Alchemic In→Sn exchange:

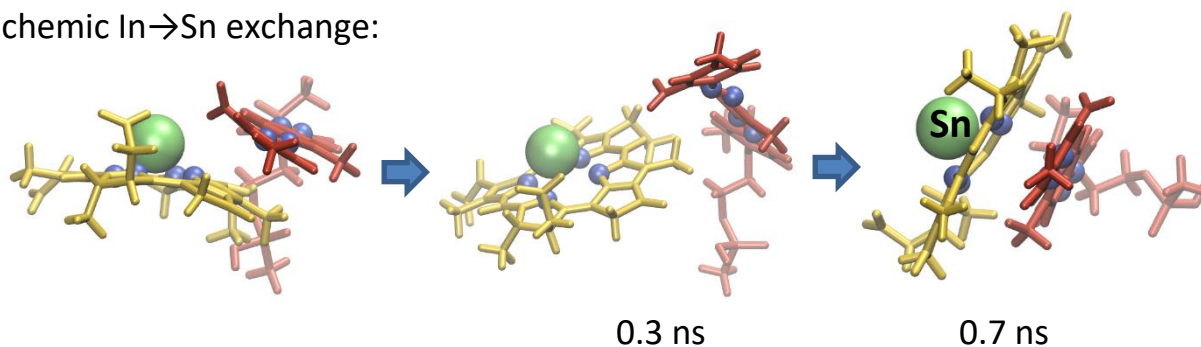


Figure S24. Evolution of a lateral PS-BHQ agglomerate taken from the In(III)-based PS complex, but replacing the metal ion by Sn(IV).

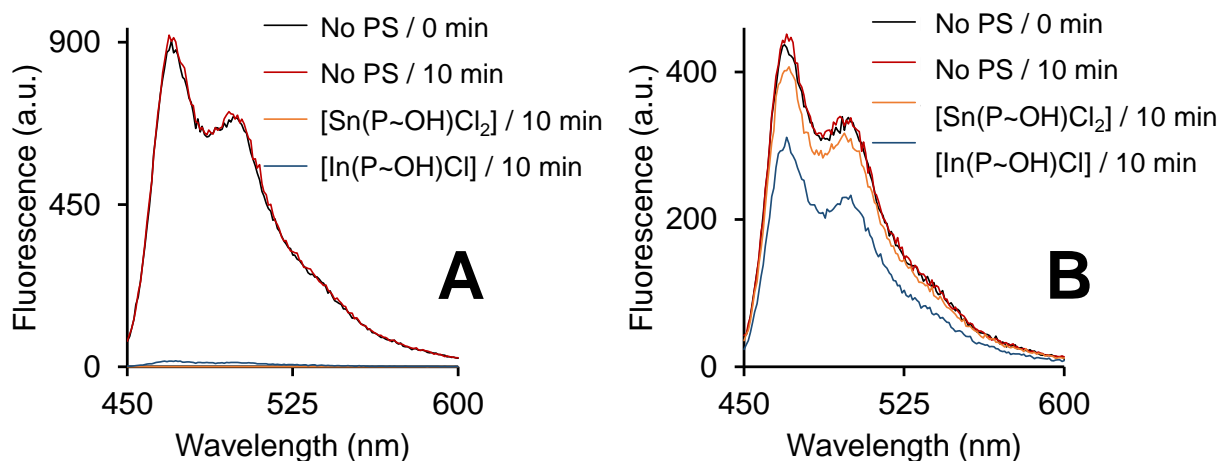


Figure S25. A: Fluorescence spectra of freshly prepared isobenzofurane (IBF) solution ($\lambda_{\text{ex}}= 430 \text{ nm}$, $25 \mu\text{M}$, “no PS/0 min”); after its irradiation with red light for 10 min in the absence of any PS (“no PS/10 min”), in the presence of either Sn(PS~OH)Cl₂ ($2 \mu\text{M}$, “Sn(PS~OH)Cl₂/10 min”) or In(PS~OH)Cl ($2 \mu\text{M}$, “In(PS~OH)Cl/10 min”). Buffer: phosphate (10 mM, pH 7), NaCl (150 mM) and DMSO (1 %, v/v). B: The same as in inset A, except that all solutions contained also sodium ascorbate (10 mM).

To explore the scope of applicability of $[\text{Sn}(\text{P}\sim\text{OH})\text{Cl}_2]$, we tested whether it can act as a catalyst of photoreduction of other organic substrates. We selected fluorescein (F), which can be reduced to its non-fluorescent leuco-form (fluorescin, FH_2), and nonfluorescent 3-azido-7-(4-methylpiperazin-1-yl)coumarin (C-N_3), which can be reduced to the corresponding fluorescent amine C-NH_2 . The reactions were conducted at different concentrations of $[\text{Sn}(\text{P}\sim\text{OH})\text{Cl}_2]$ (2-100 μM) and in the presence of different sources of electrons: ethylenediaminetetracetic acid (EDTA), sodium ascorbate and glutathione (GSH) and their combinations. We found that photoreduction of both substrates in the presence of $[\text{Sn}(\text{P}\sim\text{OH})\text{Cl}_2]$ and upon irradiation with red light is possible (Figure S22). However, to observe efficient photoreduction, we had to apply a substantial excess of the catalyst (10 eq), whereas the reduction of BHQ2-R and BHQ1-R occurs even in the presence of only 0.2 eq catalyst. Among electron sources, ascorbate was found to be most efficient.

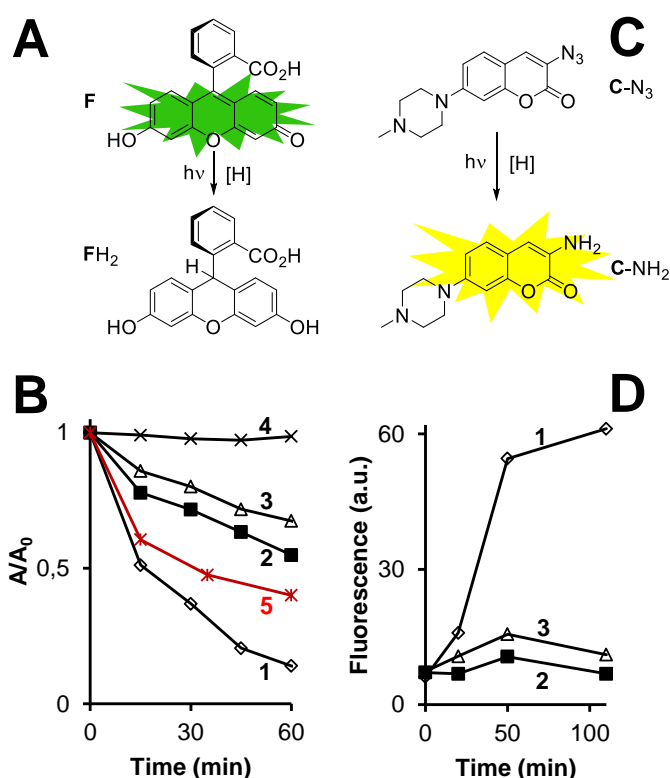


Figure S26. Scheme of photoreduction of fluorescein F (**A**) and 3-azido-7-(4-methylpiperazin-1-yl)coumarin C-N_3 (**C**) with formation of colorless fluorescin FH_2 and fluorescent C-NH_2 correspondingly. **B**: Monitoring reduction of F by UV-visible spectroscopy: A is the absorbance at 490 nm of solution of F (10 μM) in phosphate buffer (10 mM, pH 7), which was observed after “t” min (OX axis) of irradiation with red

light; A_0 is the initial absorbance at 490 nm of the same solution; mixture (1) $[\text{Sn}(\text{P}\sim\text{OH})\text{Cl}_2]$ (100 μM); ethylenediaminetetracetic acid (EDTA, 1 mM); (2) $[\text{Sn}(\text{P}\sim\text{OH})\text{Cl}_2]$ (100 μM); glutathione (GSH, 5 mM); (3) $[\text{Sn}(\text{P}\sim\text{OH})\text{Cl}_2]$ (100 μM); EDTA (1 mM); GSH (5 mM); (4) EDTA (1 mM); (5) $[\text{Sn}(\text{P}\sim\text{OH})\text{Cl}_2]$ (100 μM). **D:** Monitoring reduction of C-N₃ (10 μM) in phosphate buffer (10 mM, pH 7) by fluorescence spectroscopy ($\lambda_{\text{ex}}= 450 \text{ nm}$; $\lambda_{\text{em}}= 510 \text{ nm}$) in the following mixtures: (1) $[\text{Sn}(\text{P}\sim\text{OH})\text{Cl}_2]$ (100 μM); EDTA (1 mM); (2) EDTA (1 mM); (3) $[\text{Sn}(\text{P}\sim\text{OH})\text{Cl}_2]$ (100 μM).

PNA conjugate 2

Fmoc protected Rink amide resin (30 mg, 0.01mmol) was used as a solid support. The Fmoc- protected amino group was deprotected using 2 ml of 2% solution of 1,8-diazabicyclo [5.4.0] undec-7-ene (DBU) in dimethylformamide (DMF) for 30 minutes and then the resin was washed with DMF (10 x 1 mL) and DCM (5 x 1 mL) and dried. After that, Fmoc-Lys(mtt)-OH (31.2 mg, 0.05 mmol) was coupled on the rink amide resin in presence of N,N,N',N'-tetramethyl-O-(1H-benzotriazol-1-yl) uranium hexafluorophosphate (HBTU; 17 mg, 0.045 mmol), and 1-hydroxy-1H-benzotriazole (HOBT; 6.88 mg, 0.05 mol) and DIPEA (19 μL , 0.05 mmol) dissolved in anhydrous DMF (0.250 mL). The mixture was shaken for 30 minutes, then filtered, washed with DMF (10 x 1 mL) and DCM (5 x 1 mL) and dried *in vacuo* (0.01 mbar). After that, Fmoc-group in lysine was deprotected using 2 ml of a 2% solution of DBU in DMF for 30 minutes, then washed with DMF (10 x 1 mL) and DCM (5 x 1 mL) and dried. Separately, complex $\text{Sn}(\text{P}\sim\text{OH})\text{Cl}_2$ (its structure is shown in Scheme S1; 5.4 mg), N,N,N',N'-tetramethyl-O-(1H-benzotriazol-1-yl)uranium hexafluorophosphate (HBTU; 17 mg), and 1-hydroxy-1H-benzotriazole (HOBT; 7 mg) were dissolved in anhydrous DMF (100 μL) and DIPEA (3.8 μL) was added. The resulting mixture was immediately added to solid support. The slurry obtained was shaken overnight, then filtered, washed with DMF (10 x 1 mL) and DCM (5 x 1 mL) and dried *in vacuo* (0.01 mbar). Next, resin was treated with a 5 ml solution of 1% TFA in DCM for 5 minutes to deprotect the mtt group then washed with DCM (3 x 1 mL). The process was repeated for 5 times. After that, PNA stand was synthesized manually on the solid support by using PNA monomer (Link technology, UK). In particular, 72.5 mg of Fmoc-PNA-A(Bhoc)-OH, 34 mg of HBTU, 14 mg of HOBT was dissolved in anhydrous DMF (500 μL) and 38 μL of DIPEA was added. The mixture was added to the solid support and shaken for 30 minute and then filtered, washed with

DMF (5 x 1 mL). The coupling process was repeated one more time. After that the Fmoc was deprotected by using 1ml of 2% DBU in DMF for 30 min and the resin was washed with DMF (5 x 1 mL). Using same protocol all other PNA monomers (Fmoc-PNA-T-OH(50.6 mg), Fmoc-PNA-C(Bhoc)-OH (70.1 mg), Fmoc-PNA-G(Bhoc)-OH (74 mg)) were couple on the solid support.

Finally, Fmoc-Lys (Boc)-OH (62 mg) was coupled using the protocol to the solid support to increase the water solubility of the PNA and Fmoc group was deprotected by using 1ml of a 2% DBU in DMF for 30 min. The conjugate was cleaved from the solid support by using 1 ml of 100% TFA for 2 hr at 22 °C and the PNA was precipitated by adding 5 ml cold diethyl ether. The precipitated PNA was washed two times with cold diethyl ether (5 mL) and then dried *in vacuo* (0.01 mbar). The conjugate was purified by HPLC using the gradient of solution B (0.1% TFA in CH₃CN) in solution A (0.1 % TFA in water): from 0 to 1 min at 10 % B, in 10 min to 15 % B, in 25 min 25 % and in 35 min 50%. The HPLC profile of the analytically pure (>90 % purity) conjugate **2** is shown in Figure S27. The PNA conjugate was not detectable by either MALDI or ESI mass spectrometry. We used analytical HPLC and UV-Vis spectroscopy (Figure S28) with known extinction coefficient of Sn(P-OH)Cl₂ ($\epsilon_{430} = 45000 \text{ M}^{-1}\text{cm}^{-1}$) and PNA ($\epsilon_{260(\text{PNA}+\text{Sn}(\text{P-OH})\text{Cl}_2)} = (57800+10000) \text{ M}^{-1}\text{cm}^{-1} = 67800 \text{ M}^{-1}\text{cm}^{-1}$) to calculate the purity of the conjugate. $\epsilon_{260}/\epsilon_{430} = 1.50$, A_{260}/A_{430} (from UV-Vis Spectroscopy) = $24.15/14/.87 = 1.63$

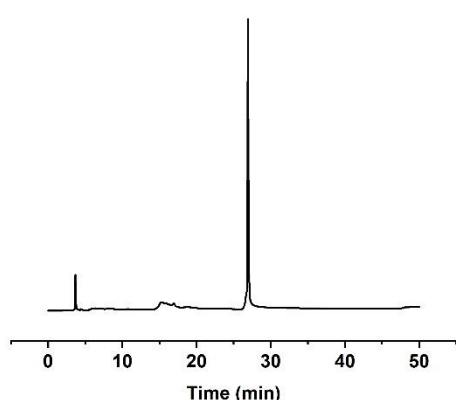


Figure S27. HPLC profile of conjugate **2**.

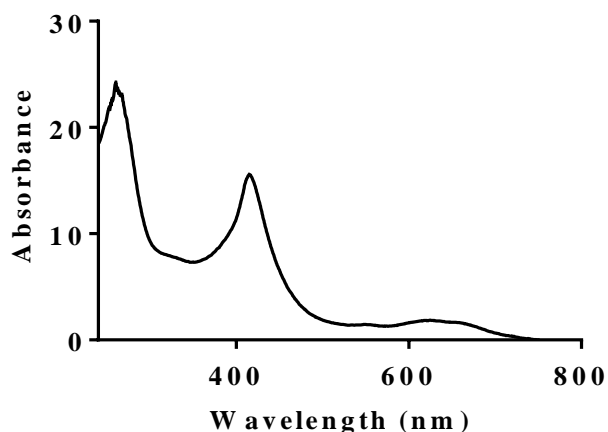


Figure S28: UV-Vis spectra of conjugate **2**.

Synthesis of substrates for the templated reaction

Solid support 3'-TAMRA CPG 1000 L (Link Technologies, UK) was used. The DNA strand was synthesized at standard conditions using a DNA synthesizer. This material ODN2~TMR~CPG was split in three portions, which are used for preparation of **3a**, **3b** and **4**.

Conjugate 3a

BHQ1-phosphoramidite (Link Technologies, UK) was coupled on the ODN2~TMR~CPG using a DNA synthesizer in accordance with manufacturer recommendations. The resulting conjugate was cleaved from the solid support and deprotected by the treatment with aqueous ammonia solution (25 %) for 2 h at 55 °C. After ammonia removal and 5-fold dilution of the mixture with water, it was purified by HPLC using the gradient of solution B (CH₃CN) in solution A ((Et₃NH)(OAc), 0.1 M in water with 5% CH₃CN): in 2 min to from 0 to 2 % B, in 32 min to 55% B. HPLC profile of analytically pure conjugate is shown in Figure S29 (left plot). This conjugate was identified by MALDI-TOF mass spectrometry in negative mode shown in Figure 29 (right plot): calculated for C₁₅₄H₁₈₈N₃₇O₇₈P₁₁ ([M-H]⁻), *m/z* 4143.8996; found 4146.5466).

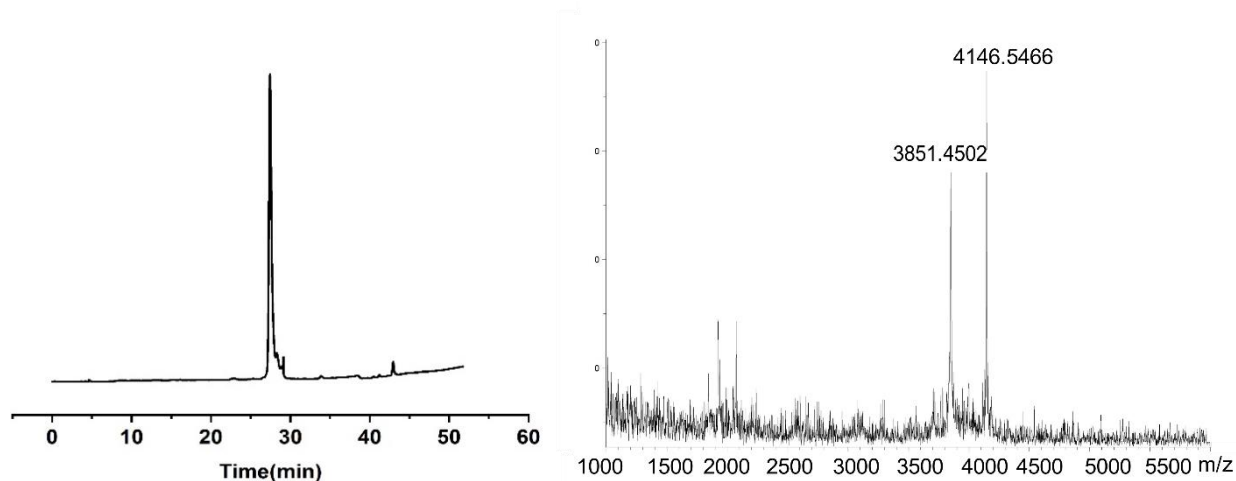


Figure S29. HPLC profile and MALDI-TOF mass spectra of conjugate **3a**.

Conjugate 3b

Phosphoramidite **S4** was coupled on solid support ODN2~TMR~CPG, synthesized as described above, manually over 10 min using solution obtained by mixing solution of **S4** in anhydrous acetonitrile (0.1 M, 0.1 mL) and solution of ETT activator in acetonitrile (0.5 M, 0.1 mL). Afterwards the solution mixture was removed, the solid support washed with anhydrous acetonitrile and the coupling was repeated. On the DNA synthesizer oxidation, capping and DMT-deprotection was performed under standard conditions of solid phase DNA synthesis. 6-FAM phosphoramidite (Link Technologies, UK) was then coupled similarly to coupling of **S4** and then oxidation and DMT-deprotection was performed again on the DNA synthesizer. Cleavage from the solid support and deprotection was performed by the treatment with a solution of t-buthylamine/MeOH/water 1:1:2 (v/v/v) for 2 h at 55 °C. After removal of t-buthylamine and MeOH the crude mixture was diluted with water and purified by HPLC using the gradient of solution B (CH₃CN) in solution A ((Et₃NH)(OAc), 0.1 M in water with 5% CH₃CN): in 5 min from 0 to 15 % B, from 15 min until 20 min to 20% B, from 30 min until 45 min to 30% B. HPLC profile of analytically pure conjugate is shown in Figure 30 (left plot). It was identified by MALDI-TOF mass spectrometry in negative mode shown in Figure S30 (right plot): calculated for C₁₇₂H₂₀₂N₃₄O₈₆P₁₂ ([M-H]⁻), *m/z* 4490.9330; found 4493.5015).

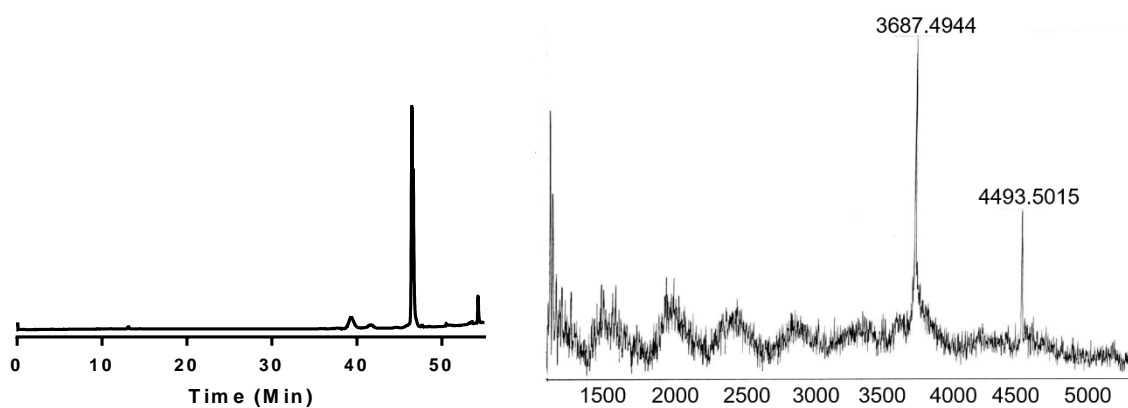


Figure S30. HPLC profile and MALDI-TOF mass spectra of conjugate **3b**.

Conjugate 4

Solid support DNA~TMR~CPG, prepared as described above, was cleaved and deprotected by the treatment with aqueous ammonia solution (25 %) for 2 h at 55 °C. After ammonia removal and 5-fold dilution of the mixture with water, it was purified by HPLC using the gradient of solution B (CH₃CN) in solution A ((Et₃NH)(OAc), 0.1 M in water with 5% CH₃CN): from 0 to 2 min at 2 % B, in 32 min to 55 % B. HPLC profile of analytically pure conjugate is shown in Figure S31 (left plot). It was identified by MALDI-TOF mass spectrometry in negative mode shown in Figure S31 (right plot): calculated for C₁₂₉H₁₆₁N₃₁O₇₂P₁₀ ([M-H]⁻), *m/z* 3606.5546; found 3606.8555).

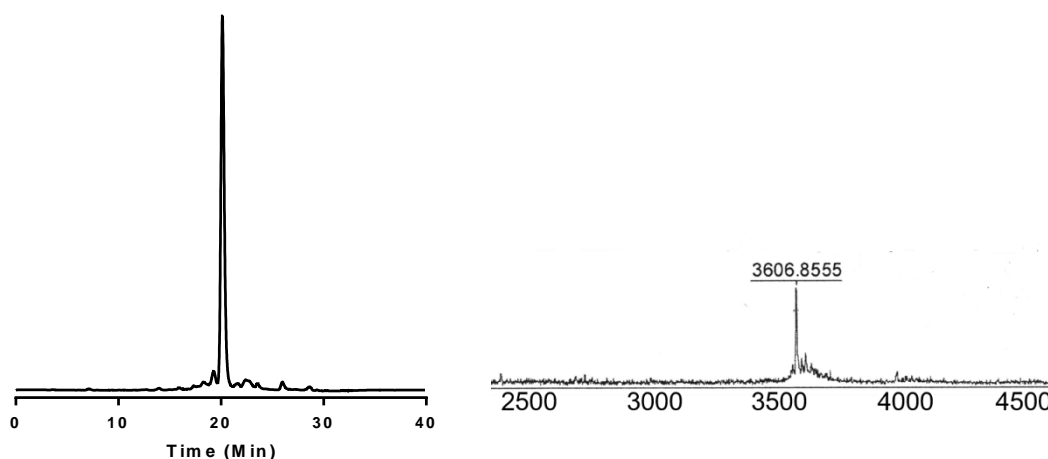


Figure S31. HPLC profile and MALDI-TOF mass spectra of conjugate **4**.

Monitoring the cleavage of the azobenzene fragments in conjugates 3a and 3b

The cleavage of azobenzene fragment in conjugate 3a and conjugate 3b after irradiation with red light in presence of [Sn(P~OH)Cl₂] or [In(P~OH)Cl] was monitored by fluorescence spectroscopy. Sodium ascorbate (10 mM) was used as reducing agent. Conjugate 3a (100 nM), photocatalyst [Sn(P~OH)Cl₂] (4 μM, 2 μM, 1 μM, 500 nM or 250 nM) or [In(P~OH)Cl] (4 μM) were mixed together in phosphate buffer (10 mM, pH 7) containing NaCl (150 mM), sodium ascorbate (10 mM) and 1% DMSO. For conjugate 3b (100 nM), photocatalyst [Sn(P~OH)Cl₂] (4 μM) or [In(P~OH)Cl] (4 μM) was used in phosphate buffer (10 mM, pH 7, NaCl 150 mM, sodium ascorbate 10 mM) containing 1% DMSO. After that, these mixtures were irradiated with red light ($\lambda = 650$ nm) and the increase of fluorescence intensity of TMR-dye ($\lambda_{\text{ex}} = 550$ nm, $\lambda_{\text{em}} = 580$ nm) was observed for both 3a and 3b conjugates and fluorescence intensity of FAM-dye ($\lambda_{\text{ex}} = 490$ nm, $\lambda_{\text{em}} = 520$ nm) was monitored for conjugate 3b. A mixture without any photosensitizer was used as a control.

Monitoring templated reactions

DNA conjugate 3a labeled at 3' end with a fluorophore (TMR) and 5' end with a quencher BHQ1 was used as a substrate, whereas, PNA conjugate 2 labeled at C- terminus with a photosensitizer [Sn(P~OH)Cl₂] was used as a photocatalyst in the nucleic acids templated reaction. Sodium ascorbate (10 mM) was used as reducing agent. In the templated reaction, the substrate, the photocatalyst and a 16 mer DNA template (a model of β actin mRNA, DNA2, Scheme 3, main text of the paper) were mixed together in phosphate buffer (10 mM, pH 7.4) containing NaCl (150 mM) and sodium ascorbate (10 mM) and allowed to stand for 30 min at 22 °C to achieve hybridization of all strands. Next, these mixtures were irradiated with red light and the increase of fluorescence intensity of TMR-dye ($\lambda_{\text{ex}} = 550$ nm, $\lambda_{\text{em}} = 580$ nm) was observed. The control mixtures lacking either the DNA template or the PNA were also included.

We evaluated the effect of single point mutations within the DNA2 template on rate of the templated reaction. In particular, we used the following mismatch DNA templates in place of DNA2: DNA2-mm1 (mutation G6 \rightarrow C6) and DNA2-mm1 (mutation G9 \rightarrow C9). Additionally, we tested effects of a gap within the DNA template (0, 1, 2, and 3 T-nucleotides) on rate of the templated reaction.

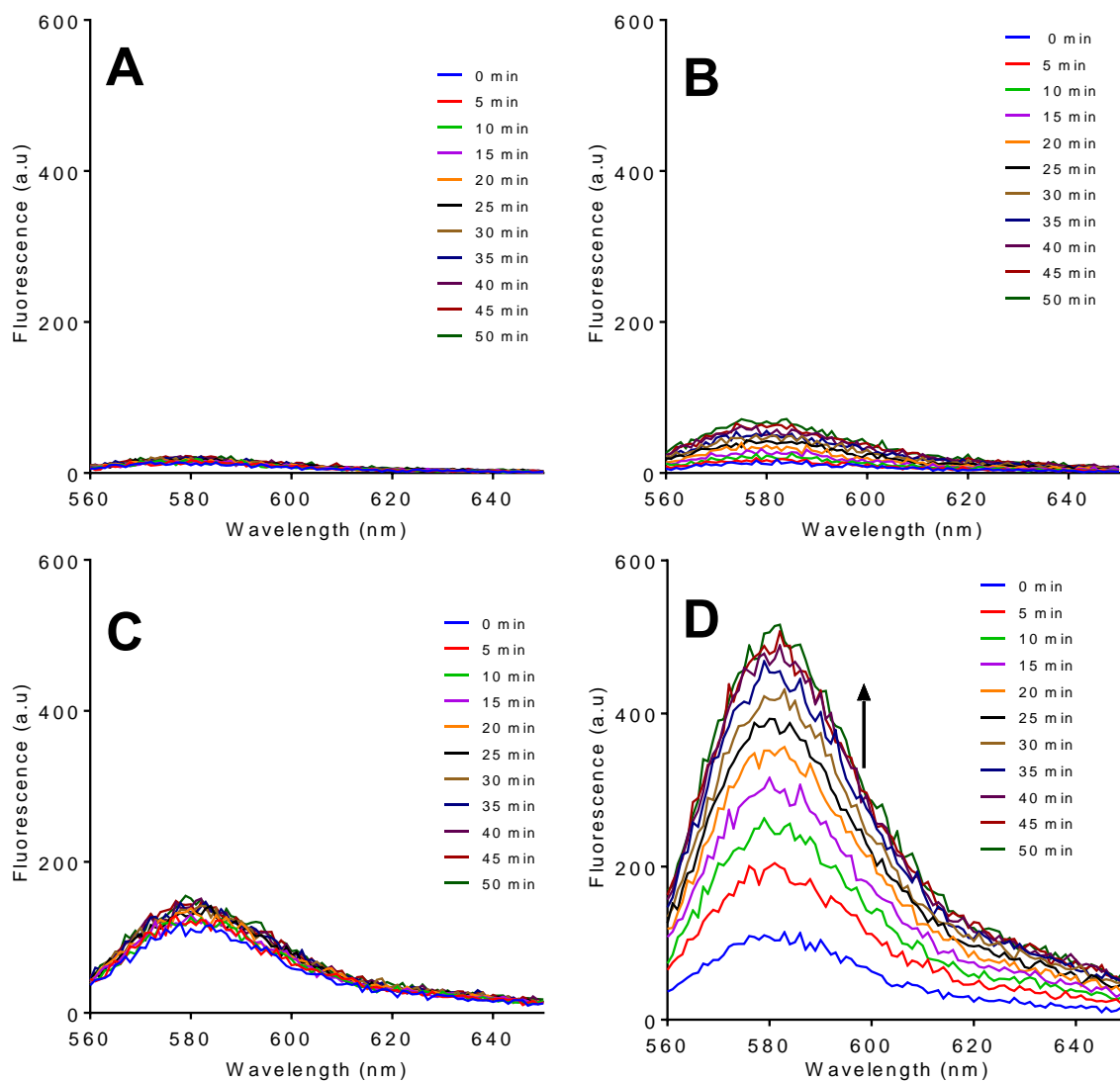


Figure S32: Representative fluorescence emission spectra ($\lambda_{\text{ex}}= 550 \text{ nm}$) of either solutions of (A) 3a (100 nM) (B) 3a (100 nM) containing PNA conjugate 2 (1eq); (C) 3a (100 nM) containing DNA2 (1eq); or (D) 3a (100 nM) containing 2 (1eq) and DNA 2(1eq) in phosphate buffer (10 mM, pH 7.0) containing NaCl (150 mM), sodium ascorbate, (10 mM). The solutions were irradiated with red light and fluorescence emission spectra was measured at different time point of irradiation (0 to 50 min). All experiments were repeated three times.

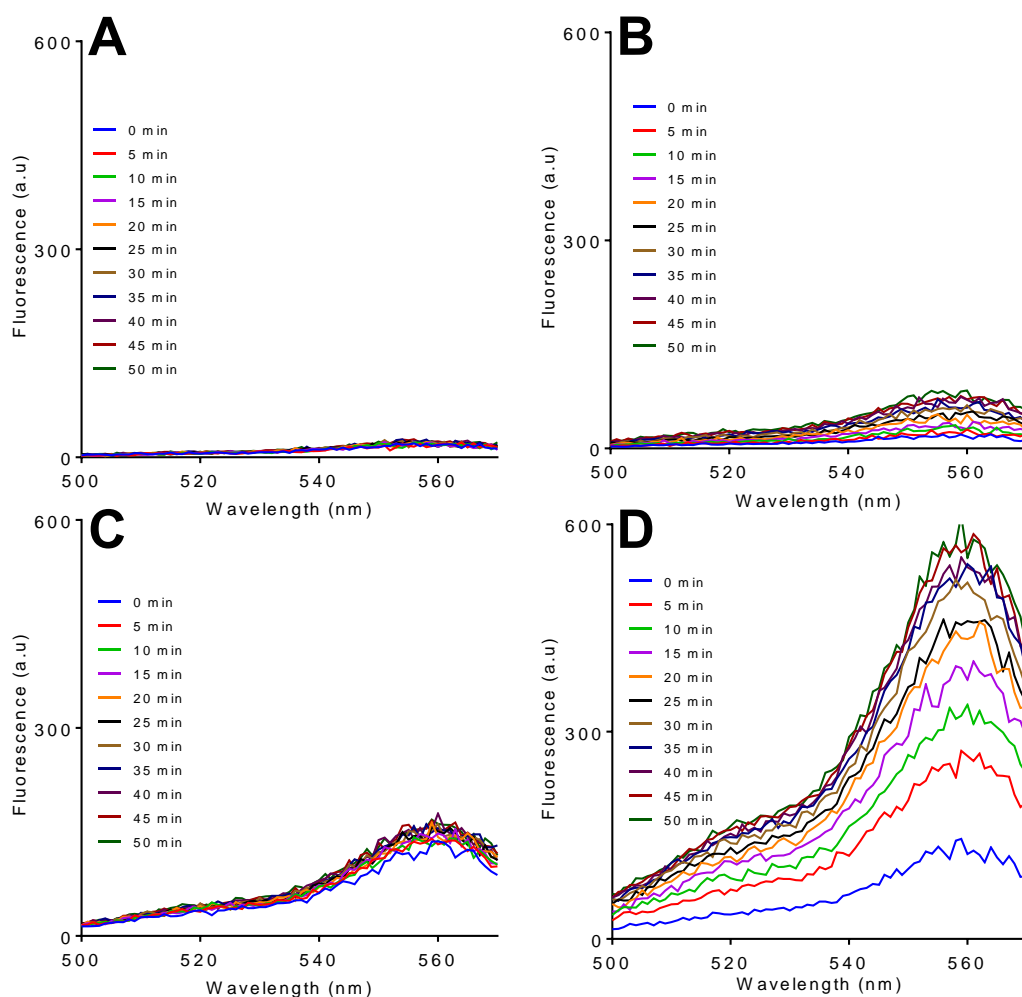


Figure S33: Representative fluorescence excitation spectra ($\lambda_{em}= 580$ nm) of either solutions of **(A)** 3a (100 nM) **(B)** 3a (100 nM) containing PNA conjugate **2** (1eq); **(C)** 3a (100 nM) containing DNA2 (1eq); or **(D)** 3a (100 nM) containing **2** (1eq) and DNA 2(1eq) in phosphate buffer (10 mM, pH 7.0) containing NaCl (150 mM), sodium ascorbate, (10 mM). The solutions were irradiated with red light and fluorescence excitation spectra was measured at different time point of irradiation (0 to 50 min). All experiments were repeated three times.

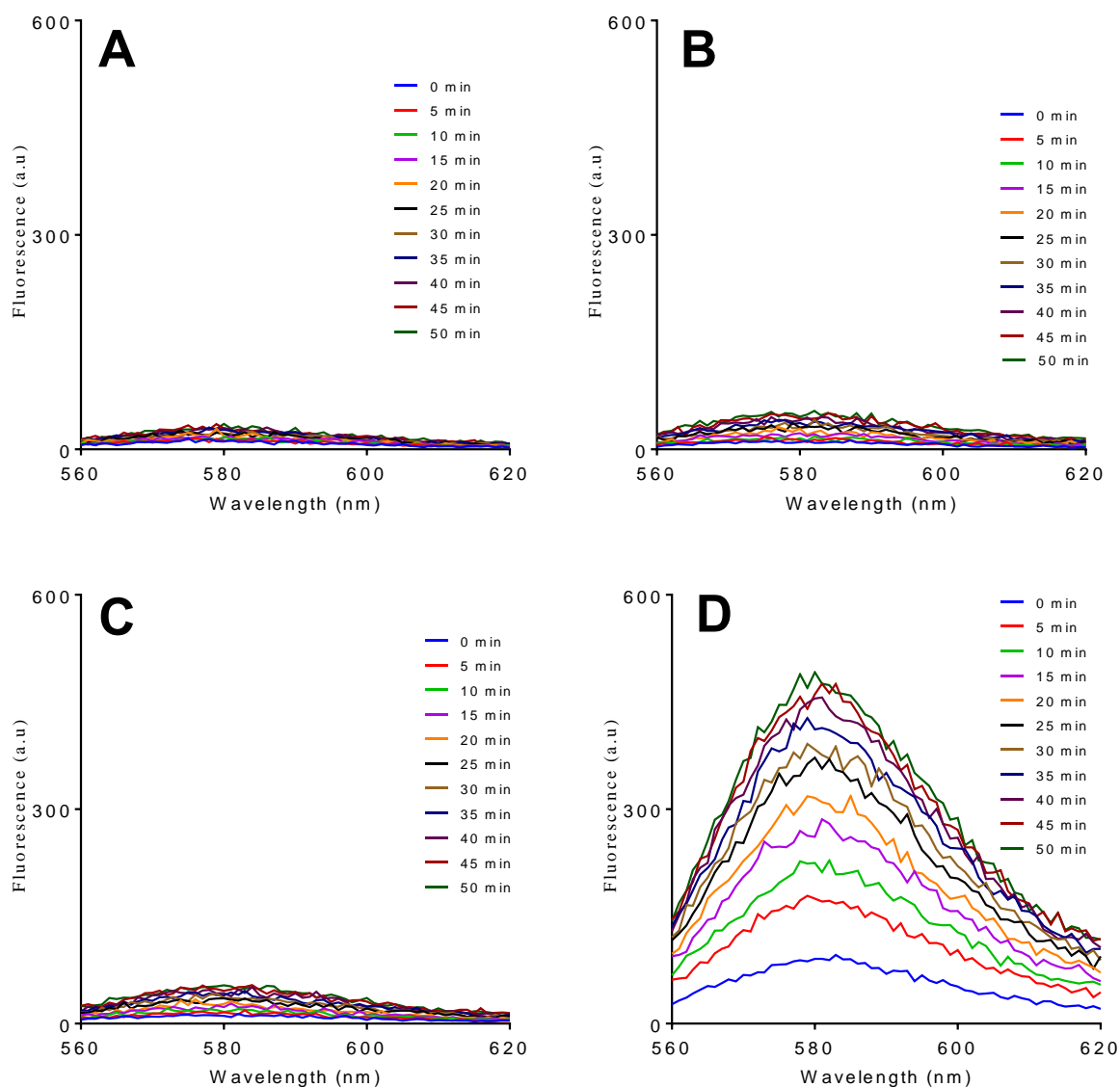


Figure S34: Representative fluorescence emission spectra ($\lambda_{ex}= 550$ nm) of either solutions of (A) 3a (100 nM); (B) 3a (100 nM) containing PNA conjugate 2 (100 nM) and DNA2-mm1 (100 nM); (C) 3a (100 nM) containing PNA conjugate 2 (100 nM) and DNA2-mm2 (100 nM); or (D) 3a (100 nM) containing PNA conjugate 2 (100 nM) and DNA2 (100 nM) in phosphate buffer (10 mM, pH 7.0) containing NaCl (150 mM) and sodium ascorbate, (10 mM). The solutions were irradiated with red light and fluorescence emission spectra was measured at different time point of irradiation (0 to 50 min). All experiments were repeated three times.

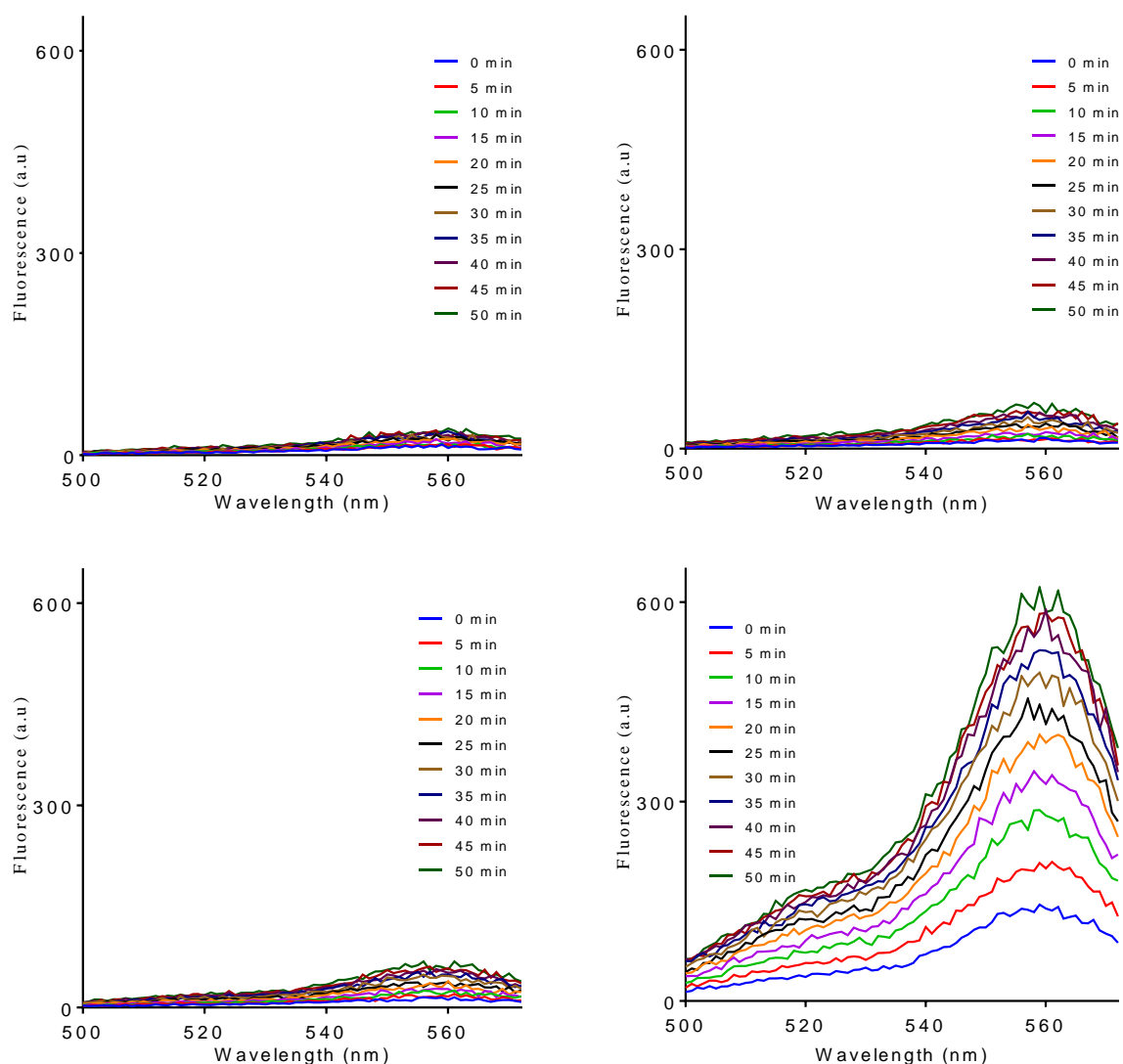


Figure S35: Representative fluorescence excitation spectra ($\lambda_{em} = 580$ nm) of either solutions of **(A)** 3a (100 nM); **(B)** 3a (100 nM) containing PNA conjugate 2 (100 nM) and DNA2-mm1 (100 nM); **(C)** 3a (100 nM) containing PNA conjugate 2 (100 nM) and DNA2-mm2 (100 nM); or **(D)** 3a (100 nM) containing PNA conjugate 2 (eq) and DNA2 (100 nM) in phosphate buffer (10 mM, pH 7.0) containing NaCl (150 mM), sodium ascorbate, (10 mM). The solutions were irradiated with red light and fluorescence excitation spectra was measure at different time point of irradiation (0 to 50 min). All experiments were repeated three times.

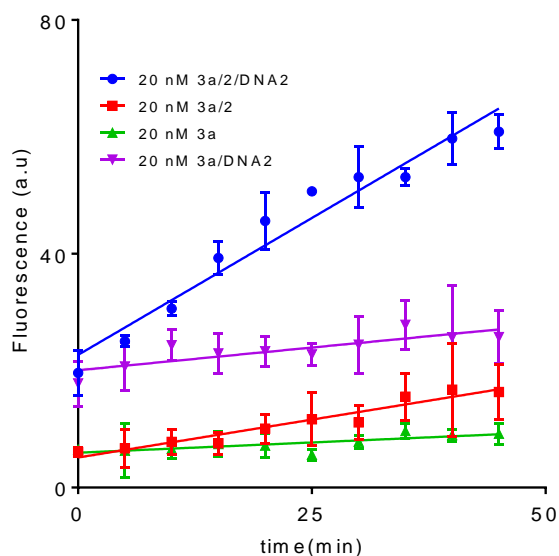


Figure S36: Kinetics of fluorescence excitation intensity of TMR ($\lambda_{em}= 580$ nm, $\lambda_{ex}= 550$ nm) upon irradiation with red light of either solutions of (A) 3a (20 nM) (green); 3a (20 nM) and PNA conjugate 2 (20 nM) (red); 3a (20 nM) and DNA2 (20 nM) (violet); 3a (20 nM), PNA conjugate 2 (20 nM) and DNA2 (20 nM) (blue) in phosphate buffer (pH 7.0) containing 150 mM NaCl and 10 mM ascorbate.

Table S1. Templated photoreduction of 3a in the presence of 20 nM DNA2.ⁱ

Reaction mixture	(dF/dt) _{t=0} , a.u. / min
3a (20 nM)	0.07 ± 0.02
3a (20 nM) / 2 (20 nM)	0.26 ± 0.04
3a (20 nM) / DNA2 (20 nM)	0.15 ± 0.05
3a (20 nM) / 2 (20 nM) / DNA2 (20 nM)	0.94 ± 0.05

ⁱ Photochemical reduction of S1 substrate in conjugate 3a (20 nM) dissolved in phosphate buffer (10 mM, pH 7) containing NaCl (150 mM) and sodium ascorbate (10 mM) in the presence of 2 (20 nM) and DNA2 template (20 nM). The mixtures were irradiated with red light for up to 50 min and their fluorescence was measured: $\lambda_{ex}= 550$ nm, $\lambda_{em}= 580$ nm. The dependence of the fluorescence increase (a.u.= arbitrary units) *versus* time (min) was fitted with a linear function to determine the initial fluorescence increase: (dF/dt)_{t=0},

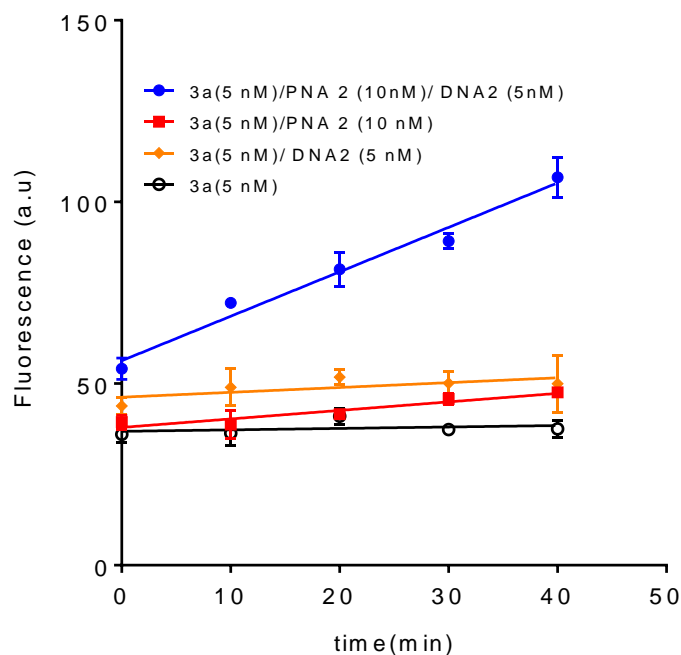


Figure S37: Kinetics of fluorescence excitation intensity of TMR ($\lambda_{em}= 580$ nm, $\lambda_{ex}= 550$ nm) upon irradiation with red light of either solutions of (A) 3a (5 nM) (black); 3a (5 nM) and PNA conjugate 2 (10 nM) (red); 3a (5 nM) and DNA2 (5 nM) (orange); 3a (5 nM), PNA conjugate 2 (10 nM) and DNA2 (5 nM) (blue) in phosphate buffer (pH 7.0) containing 150 mM NaCl and 10 mM ascorbate.

Table S2. Templated photoreduction of 3a in the presence of 5 nM DNA2.[†]

Reaction mixture	(dF/dt) _{t=0} , a.u. / min
3a (5 nM)	0.04 ± 0.05
3a (5 nM) / 2 (10 nM)	0.23 ± 0.04
3a (5 nM) / DNA2 (5 nM)	0.13 ± 0.08
3a (5 nM) / 2 (10 nM) / DNA2 (5 nM)	1.22 ± 0.08

[†] Photochemical reduction of S1 substrate in conjugate 3a (5 nM) dissolved in phosphate buffer (10 mM, pH 7) containing NaCl (150 mM) and sodium ascorbate (10 mM) in the presence of 2 (10 nM) and DNA2 template (5 nM). The mixtures were irradiated with red light for up to 50 min and their fluorescence was measured: $\lambda_{ex}= 550$ nm, $\lambda_{em}= 580$ nm. The dependence of the fluorescence increase (a.u.= arbitrary units) *versus* time (min) was fitted with a linear function to determine the initial fluorescence increase: (dF/dt)_{t=0},

References

- S1. J. Wang, R. M. Wolf, J. W. Caldwell, D. A. Case, *J. Comput. Chem.*, 2004, **25**, 1157.
- S2. C. I. Bayly, P. Cieplak, W. D. Cornell, P. A. Kollman, *J. Phys. Chem.*, 1993, **97**, 10269.
- S3. P. Li, K. Merz, *J. Chem. Theory Comput.*, 2014, **10**, 289.
- S4. P. Li, L. Song, K. Merz, *J. Phys. Chem. B*, 2015, **119**, 883.
- S5. Z. Wu, H. L. Tepper, G. A. Voth, *J. Chem. Phys.*, 2006, **124**, 024503.